lesions, including those caused by oxidative damage such as strand breaks, base modification, and abasic sites, will block the progression of the polymerase, resulting in a decrease in amplification of the intact mitochondrial genome.

FCS sensitively measures fluctuations in fluorescence intensity generated by only a few fluorescent molecules diffusing in and out of an extremely tiny volume element at the subfemtoliter level in solution. The characteristics of the fluctuations are dependent on the base length and the concentration [8–10]. Thus, FCS probably detects a decrease in the LPCR product, which has the same base length as intact mtDNA. Furthermore, because of the short analysis time and the economic efficiency of the small sample volume, FCS would be advantageous for massive specimen analysis [9].

The purpose of this study was to test the feasibility of detecting mtDNA damage caused by oxidative stress using the LPCR–FCS method. After human embryonic kidney 293 (HEK-293) cells, used as test cells, were treated with different concentrations of H_2O_2 for 60 min, total cellular DNA was extracted. The mtDNA genome was amplified by LPCR and the product was confirmed with restriction enzymes. We added the fluorescent dye YOYO-1 to the LPCR medium to detect fluorescence fluctuations resulting from both the LPCR products and primer. Fluorescence autocorrelation functions were analyzed using a two-component model, and the optimal amount of template DNA was determined first. Then the dependence of the fraction of the LPCR product on H_2O_2 was evaluated.

Materials and methods

Cell culture

HEK-293 cells were grown in a 5% CO_2 humidified atmosphere at 37 °C in Dulbecco's modified Eagle's medium (DMEM) supplemented with 10% fetal bovine serum, 2×10^5 U/L penicillin G, and 200 mg/L streptomycin sulfate. The cells were routinely split every 3–4 days, and 10^6 cells were plated in 60-mm dishes 14–16 h before exposure to 0–0.4 mM H_2O_2 for 60 min [1]. Then the cells were washed once with phosphate-buffered saline (PBS) and harvested immediately by brief trypsinization (0.25%).

DNA isolation and LPCR

Using a GeneBall DNA isolation kit (TaKaRa, Japan), 30 μg of total cellular DNA was extracted from 10^6 cells. The concentration of total cellular DNA was determined by absorption at 260 nm with a SmartSpec 3000 spectrophotometer (Bio-Rad, USA). The primer nucleotide sequences were as follows: for the 16.2-kb fragment of the mitochondrial genome, the forward primer 5′-TGAG GCCAAATATCATTCTGAGGGGC-3′ and the reverse primer 5′-TTTCATCATGCGGAGATGTTGGATGG-3′ [7]; for the 17.6-kb fragment upstream of the nuclear β-globin gene (GenBank, NG_000007), the forward primer 5′-TGCACCTGCTCTGTGATTATGACTATCCCACA GTC-3′ and the reverse primer 5′-ACATGATTAGCA AAAGGGCCTAGCTTGGACTCAGA-3′. The β-globin gene encoded in the nuclear chromosome was used as a control to confirm mtDNA-specific damage.

LPCR were performed in a PC707 thermal cycler (Astec, Japan) using a TaKaRa LA Taq PCR kit as described by the manufacturer. The thermal cycle profile was as follows: initial denaturation for 1 min at 94 °C, followed by 20 cycles for mtDNA or 24 cycles for β-globin at 94 °C denaturation for 30 s and 68 °C primer extension for 15 min. A final extension at 72 °C was performed for 10 min at the completion of each profile. To confirm the LPCR product, parts of the product were digested with four restriction enzymes: *Eco*47I (TaKaRa), *Hae*III (TaKaRa), *Hga*I (New England BioLabs, USA), and *Bsp*MI (New England BioLabs). Each digest was analyzed on gel.

Fluorescence spectra of YOYO-1

The fluorescent cyanine dye YOYO-1 was purchased from Molecular Probes (USA). LPCR product–YOYO-1 complexes were made by mixing equal volumes of LPCR medium and 1 μM YOYO-1 in 10 mM Tris (pH 7.4). The mixed solution was incubated at room temperature for 30 min before use. Fluorescence spectra of YOYO-1 solution (0.5 μM) were recorded with an FP6500 fluorescence spectrophotometer (Jasco, Japan).

FCS measurement

FCS measurement was performed using a ConfoCor fluorescence correlation measurement system (Carl Zeiss Jena, Germany), as described elsewhere [11]. A sample droplet (20 μl) was set on a cover glass and was excited with approximately 10 kW/cm^2 of laser power (Ar^+) at 488 nm. The fluorescence signal was detected through a dichroic mirror (>510 nm) and a bandpass filter (515–560 nm). Measurements were conducted at room temperature.

Theoretical works on fluorescence correlation spectroscopy have been published previously by various authors [12–14]. Briefly, because fluorescence intensity fluctuates with only a few fluorescent molecules diffusing in and out of the volume element, the fluorescence intensity at time t, $I(t)$, changes into $I(t+\tau)$ τ seconds later. The fluorescence autocorrelation function is calculated from a random fluctuation of fluorescence intensity as follows:

$$G(\tau) = \frac{\langle I(t) \times I(t+\tau) \rangle}{\langle I(t) \rangle^2}. \quad (1)$$

The typical shape of an autocorrelation in Eq. (1) usually has high amplitude for time ranges shorter than approximately 1 ms and almost no amplitude for time ranges longer than approximately 1 ms. This suggests that every molecule that gives a correlation signal occupies the

volume element for a shorter time but that only a few molecules stay for a longer time. Therefore, a high amplitude lasts when large molecules stay in the volume element for a longer time because they diffuse slowly.

In the current study, the fluorescence autocorrelation function, $G(\tau)$, was fitted to a simple two-component model, where the variables were the average number of fluorescent molecules (N), the translational diffusion time of the free fast-moving component of the primer (τ_{primer}), and the translational diffusion time of the slow-moving component of the LPCR product ($\tau_{product}$), as shown in the following equation:

$$G(\tau) = 1 + \frac{1}{N}\left[\left\{\frac{1-y}{1+\frac{\tau}{\tau_{primer}}}\sqrt{\frac{1}{1+\frac{s^2\tau}{\tau_{primer}}}}\right\} + \left\{\frac{y}{1+\frac{\tau}{\tau_{product}}}\sqrt{\frac{1}{1+\frac{s^2\tau}{\tau_{product}}}}\right\}\right], \quad (2)$$

where $\tau_{primer,product} = w_0^2/4D_{primer,product}$, $s = w_o/z_o$, y is the fraction of the slow-moving component, w_o is the radius of the detection field (volume element), $2z_o$ is the field length, D_{primer} and $D_{product}$ are the translational diffusion constants of the free fast-moving product and the slow-moving product, respectively, and s is the structure parameter. The data analysis was performed using the nonlinear least-squares fitting method with the FCS ACCESS computer program (EVOTEC BioSystems, Germany). In the current study, s (0.192) was obtained previously with rhodamine 6G as the reference standard. After determining τ_{primer} and $\tau_{product}$ (see Results and discussion later), y and N were obtained from the fitting of every autocorrelation function.

The optimal amount of template DNA was determined first, and then the effect of H_2O_2 exposure on DNA damage was evaluated by changes in fraction in FCS measurement of LPCR products for mtDNA and the β-globin gene. The results were compared with those obtained by gel electrophoresis.

Frequency of DNA lesions

Assuming a random distribution of lesions, the Poisson equation (e^{-s}, where s = lesion frequency) was used to calculate the lesion frequency per genomic strand: $s = -\ln(A_d/A_o)$ = lesion frequency/strand, where A_o = the fraction of the slow component obtained from a given amount of nondamaged DNA template and A_d = the fraction of slow component of the DNA template damaged by a particular dose of H_2O_2 [15].

Densitometric analysis after gel electrophoresis

After the LPCR mixture was applied to 1% agarose gel, the gel was stained with fluorescence dye (Gelstar, TaKaRa). Then the digital image of the gel was recorded with a CCD camera (C-3040, Olympus, Japan) under UV light. The relative abundance of the LPCR product in each sample on gel was quantified by densitometric analysis using Scion Image (Scion, USA). After background subtraction, the intensities in the band of interest were divided by the highest band intensity in each gel, and the abundance was expressed as relative band intensity.

Statistical analysis

The results were analyzed for statistical significance by the unpaired Student's t test using Microcal Origin (OriginLab, USA). Values are expressed as the means and standard errors of three to five individual experiments unless stated otherwise.

Results and discussion

LPCR products labeled with YOYO-1

Using total DNA extracted from normal cells without H_2O_2 treatment, the mtDNA genome and target sequence of β-globin were amplified by LPCR. Both products were electrophoresed and appeared as single bands near 17 kbp on the gel. These were confirmed by the digestion with four restriction enzymes, demonstrating a pattern of fragment distribution identical to that expected from the GenBank data (data not shown).

In 0.5 μM YOYO-1 solution containing the mtDNA LPCR product, intense fluorescence was observed near 510 nm, as shown in Fig. 1A. YOYO-1 alone had little fluorescence at that wavelength. When interacted with the primer for mtDNA amplification, it had weak fluorescence that was one-third the fluorescence intensity of the coexistent solution of the mtDNA LPCR product. The fluorescence spectra and the intensity of the primer for the β-globin gene and of the LPCR product were identical to those for mtDNA (data not shown). Thus, the interaction between each LPCR primer and YOYO-1 also caused fluorescence.

Diffusion time of primer and LPCR products

The fluorescence autocorrelation functions of the primer for mtDNA amplification, the LPCR products for mtDNA, and the β-globin gene are shown in Fig. 1B. The function of the mtDNA LPCR product was nearly identical to that of the β-globin LPCR product due to similar base length but was largely shifted to the right compared with that of the primer. The fluorescence autocorrelation function of the primer for β-globin gene amplification was identical to that for mtDNA (data not shown). These results suggested that the LPCR product diffused much slower than the primer due to its longer length.

By fitting the autocorrelation function of the primer for mtDNA amplification to a simple one-component model, where $y = 0$ in Eq. (2), the diffusion time was obtained (Table 1). Then the fluorescence correlation functions of the mtDNA and β-globin LPCR products were fitted to

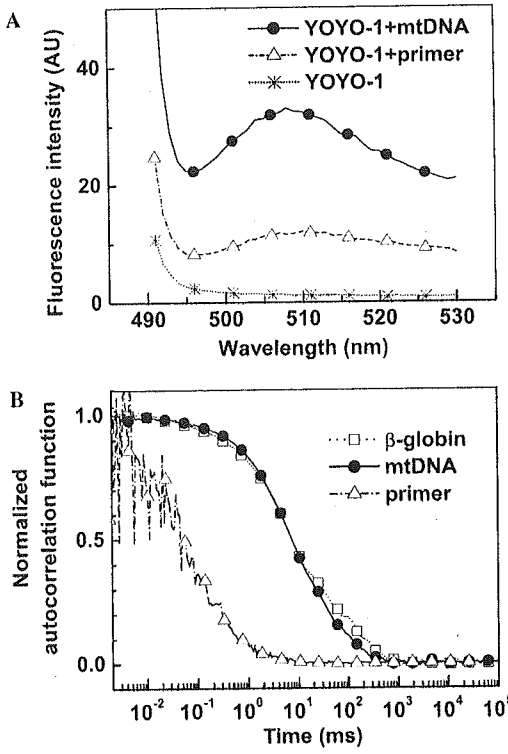

Fig. 1. (A) Fluorescence spectra (●) of 0.5 μM YOYO-1 associated with the mtDNA LPCR product, having an emission maximum at 510 nm. YOYO-1 alone (✳) had little fluorescence at the wavelength. When interacted with the primer for mtDNA amplification, it had a weak fluorescence (Δ), which was one-third the fluorescence in the solution containing the mtDNA LPCR product. (B) Typical normalized autocorrelation functions of the LPCR products of mtDNA and β-globin and the primer for mtDNA amplification.

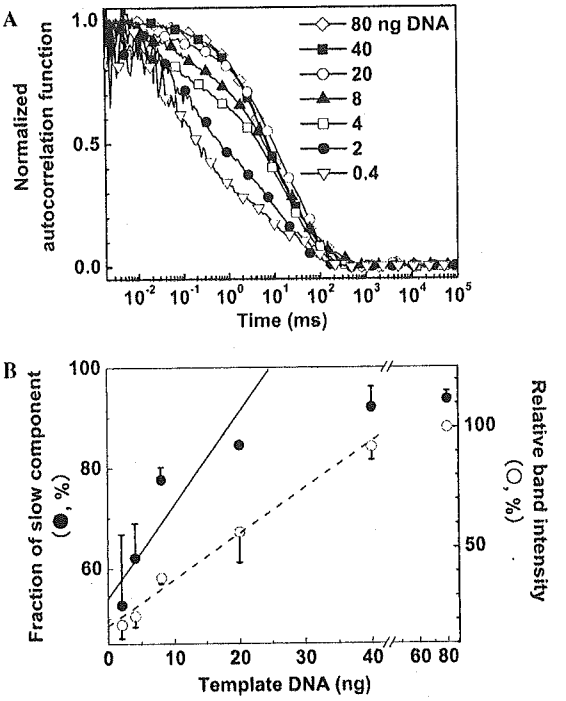

Fig. 2. (A) Changes in normalized autocorrelation functions of mtDNA LPCR products due to the amount of template DNA (0.4–80 ng). (B) Dependence of amount of template DNA on the fraction of the slow component obtained from two-component analysis of the autocorrelation function of the mtDNA LPCR product (●, means + SE) and on relative band intensity by densitometry after gel electrophoresis (○, means − SE). Regression lines are $y = 55 + 1.6x$ ($R = 0.90$) for the fraction of the slow component and $y = 17 + 1.9x$ ($R = 0.99$) for the relative band intensity (2–20 ng of total DNA).

a simple two-component model with a fast-moving component of the free primer and a slow-moving component of the LPCR product using Eq. (2). The diffusion times of the LPCR products ($\tau_{product}$) were determined by curve fitting of autocorrelation data to the two-component model and were found to be 18.2 ± 0.4 ms for mtDNA and 19.6 ± 3.3 ms for β-globin (Table 1). In the following analysis, the obtained values were considered as constant to reduce the number of free parameters.

Dependence of template DNA amount on fraction of slow component

Because the relationship between the amount of template DNA and the number of LPCR products is linear, the fraction was also expected to be dependent on the amount. As shown in Fig. 2A, the autocorrelation function of LPCR products was shifted to the left with the decrease in template DNA from 80 to 0.4 ng, showing a decrease in the slow component. When the functions were analyzed with the two-component model, the fraction of the slow component decreased consistently (Fig. 2B). At more than 20 ng, the fraction seemed to be saturated. The changes in the fraction were similar to the results obtained from densitometry (~17 kbp), although the values of the fraction in FCS were different from those of relative band intensities, which were normalized with the band intensity of 80 ng of template DNA. The results suggest that we can detect the decrease in LPCR product, caused by oxidative stress, if up to 20 ng of template DNA is used under the current conditions of LPCR.

Table 1
Diffusion time of the primer (τ_{primer}) for mtDNA amplification, LPCR products ($\tau_{product}$) for mtDNA, and β-globin

	Primer	mtDNA	β-Globin
Diffusion time (ms)	0.21 ± 0.03	18.2 ± 0.4	19.6 ± 3.3
Number of samples	5	4	3

Note. Values are expressed as means and standard errors.

Effect of H_2O_2 on fraction of slow component

Cells were treated with various concentrations of H_2O_2 up to 1 mM for 1 h. Just after exposure to 1 mM, cells detached from culture dishes. Under conditions up to 0.4 mM, cells remained attached. When cells were treated with 0.4 mM H_2O_2, cell growth was suppressed 2 days after the treatment, probably due to apoptosis [1].

After exposure up to 0.4 mM H_2O_2 for 60 min, total DNA of the cells was extracted. With 20 ng of total DNA as a template, the target sequence was amplified and FCS measurement was conducted. When 0.1 mM H_2O_2 was added, a decrease in the fraction for the mtDNA LPCR product from 79.3 ± 5.4 to 67.9 ± 3.4% was observed. At 0.4 mM, the fraction was decreased significantly to 53.9 ± 5.0% (Fig. 3A). The pattern of change was similar to the result of the gel electrophoresis, although the values of fractions obtained by FCS were different from those of relative band intensities, which were normalized with the highest band intensity in each gel. The fraction of the nuclear-encoded β-globin LPCR product remained unchanged, that is, approximately 60% under conditions up to 0.4 mM H_2O_2 (Fig. 3B). H_2O_2-induced mtDNA lesion frequency increased with its dose (Fig. 3C). The frequencies were 0.17 ± 0.07 lesions/10 kb with 0.2 mM treatment and 0.25 ± 0.05 lesions/10 kb with 0.4 mM treatment. We confirmed that there was little effect of H_2O_2 on the β-globin LPCR product on gel. The results shown in Fig. 3 were consistent with those obtained in previous studies indicating that mtDNA was more sensitive than nuclear DNA to H_2O_2 exposure [1,4]. Therefore, the results suggest that oxidative damage of mtDNA can be detected by the LPCR–FCS method.

Primary screening of oxidative stress-induced mtDNA damage

The analysis time of FCS measurement was approximately 5 min, whereas that of gel electrophoresis was more than 3 h, in the current study. The current method is proposed only for a rapid primary screening, not for accurate evaluation of oxidative damage in the mtDNA genome. When the ratio of mtDNA to the nuclear-encoded gene LPCR product is significantly low due to a decrease in the intact mtDNA genome, the screened sample from FCS can be immediately subjected to detailed analysis such as sequencing.

The current measurements of FCS were carried out with a 20-μl sample volume, although theoretically the volume can be reduced to a volume element on the order of 10^{-15} L [9]. Practically, the sample volume for LPCR can be reduced to 1 μl. Thus, this LPCR–FCS method would also have a great advantage from an economic point of view. Physical handling of such a small sample volume can be done by using a capillary tube or a small sample pit on a glass surface covered by a thin film or cover glass for mass examination.

In contrast to common methods used previously without amplification, such as Northern blotting and HPLC–electrochemical detection, target DNA was amplified in our method so that a smaller sample could be employed. Although our method has some of the same limitations as other methods with amplification (e.g., real-time PCR), the DNA sample can be reduced due to the tiny volume element. In this study, we used 20 ng of total DNA. As shown in Fig. 2B, 2 ng of total DNA was sufficient to detect the mtDNA LPCR product. Furthermore, because 30 μg of total DNA was isolated from 10^6 cells, mtDNA damage could be detected using a few hundred cells.

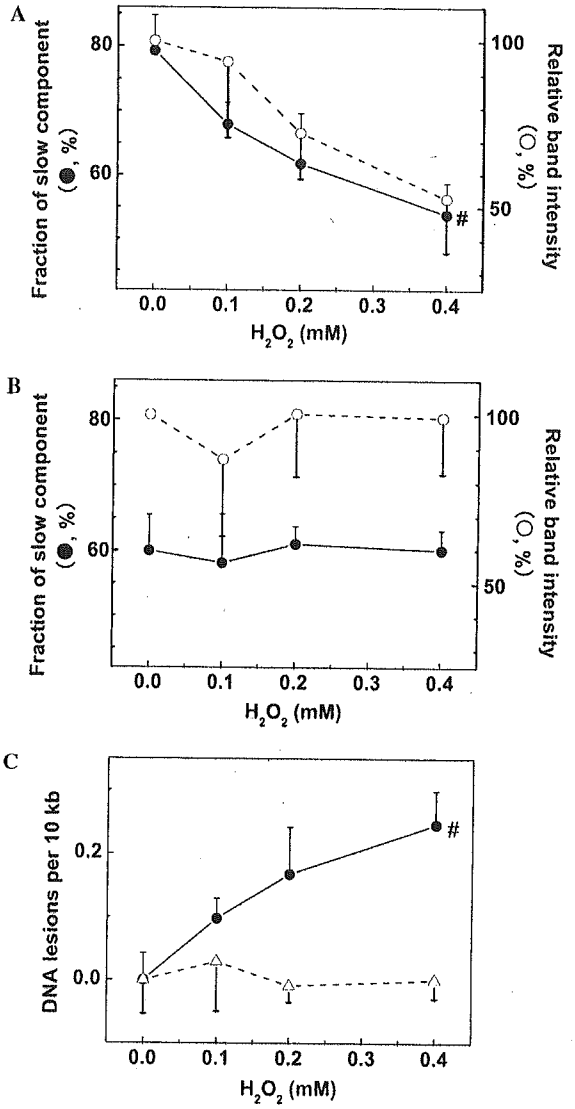

Fig. 3. (A) H_2O_2 dependence on the fraction of the slow component obtained from two-component analysis of the autocorrelation function of the mtDNA LPCR product (●, means + SE) and on relative band intensity obtained by densitometry after gel electrophoresis (○, means − SE). (B) H_2O_2 dependence on the fraction for β-globin. (C) Lesion frequencies in mtDNA (●, means + SE) and β-globin gene (Δ, means − SE), evaluated by FCS. $^{\#}P < 0.05$ compared with the fraction without H_2O_2 treatment.

Currently, real-time PCR may be the most sensitive and precise method for detection and quantification of nucleic acids. However, it is a complex technique and substantial problems are associated with its reproducibility. Furthermore, in contrast to our method measuring after PCR, the real-time PCR method measures fluorescence intensity

during PCR so that its target usually ranges from 100 to 500 bp. If real-time PCR is expanded for a long target sequence, setting the optimal PCR conditions becomes complicated. Our LPCR–FCS method makes possible the evaluation of oxidative stress-induced mtDNA damage without a complex process.

In conclusion, the current method would be advantageous for epidemiological studies to determine the relationship between mtDNA damage and the diseases in which mitochondrial deficiencies might be relevant.

Acknowledgment

This study was supported financially in part by a Grant-in-Aid for Scientific Research (C 2 14580761) from the Ministry of Education, Science, Sports, and Culture of Japan.

References

[1] F.M. Yakes, B. van Houten, Mitochondrial DNA damage is more extensive and persists longer than nuclear DNA damage in human cells following oxidative stress, Proc. Natl. Acad. Sci. USA 94 (1997) 514–519.

[2] W.J. Driggers, S.P. LeDoux, G.L. Wilson, Repair of oxidative damage within the mitochondrial DNA of RINr 38 cells, J. Biol. Chem. 268 (1993) 22042–22045.

[3] J.H. Santos, L. Hunakova, Y. Chen, C. Bortner, B. van Houten, Cell sorting experiments link persistent mitochondrial DNA damage with loss of mitochondrial membrane potential and apoptotic cell death, J. Biol. Chem. 278 (2003) 1728–1734.

[4] G. Wang, T.K. Hazra, S. Mitra, H.M. Lee, E.W. Englander, Mitochondrial DNA damage and a hypoxic response are induced by $CoCl_2$ in rat neuronal PC12 cells, Nucleic Acids Res. 28 (2000) 2135–2140.

[5] M. Deschauer, A. Krasnianski, S. Zierz, R. Taylor, False-positive diagnosis of a single, large-scale mitochondrial DNA deletion by Southern blot analysis: the role of neutral polymorphisms, Genet. Test. 8 (2004) 383–387.

[6] C. Richter, J.W. Park, B.N. Ames, Normal oxidative damage to mitochondrial and nuclear DNA is extensive, Proc. Natl. Acad. Sci. USA 85 (1988) 6465–6467.

[7] S. Cheng, R. Higuchi, M. Stoneking, Complete mitochondrial genome amplification, Nat. Genet. 7 (1994) 350–351.

[8] Y. Nomura, M. Kinjo, Real-time monitoring of in vitro transcriptional RNA using fluorescence correlation spectroscopy, ChemBioChem 5 (2004) 1701–1703.

[9] M. Kinjo, Detection of asymmetric PCR products in homogeneous solution by fluorescence correlation spectroscopy, BioTechniques 25 (1998) 706–715.

[10] M. Kinjo, R. Rigler, Ultrasensitive hybridization analysis using fluorescence correlation spectroscopy, Nucleic Acids Res. 23 (1995) 1795–1799.

[11] Y. Nomura, H. Tanaka, L. Poellinger, F. Higashino, M. Kinjo, Monitoring of in vitro and in vivo translation of green fluorescent protein and its fusion proteins by fluorescence correlation spectroscopy, Cytometry 44 (2001) 1–6.

[12] M. Kinjo, Quantitative analysis by the polymerase chain reaction using fluorescence correlation spectroscopy, Anal. Chim. Acta 365 (1998) 43–48.

[13] R. Rigler, U. Mets, J. Widengren, P. Kask, Fluorescence correlation spectroscopy with high count rate and low background: analysis of translational diffusion, Eur. Biophys. J. 22 (1993) 166–175.

[14] S. Aragon, R. Pecora, Fluorescence correlation spectroscopy as a probe of molecular dynamics, J. Chem. Phys. 64 (1976) 1791–1803.

[15] D.P. Kalinowski, S. Illenye, B. Van Houten, Analysis of DNA damage and repair in murine leukemia L1210 cells using a quantitative polymerase chain reaction assay, Nucleic Acids Res. 20 (1992) 3485–3494.

Expert Opinion

Ashley Publications
www.ashley-pub.com

Gene Therapy

Gene therapy for Parkinson's disease using recombinant adeno-associated viral vectors

Shin-ichi Muramatsu†, Hideo Tsukada, Imaharu Nakano & Keiya Ozawa
†Jichi Medical School, Division of Neurology, Department of Medicine, 3311-1 Yakushiji, Minami-kawachi, Tochigi, 3290498 Japan

Existing strategies for gene therapy in the treatment of Parkinson's disease include the delivery of genes encoding dopamine (DA)-synthesising enzymes, leading to localised production of DA in the striatum; genes encoding factors that protect nigral neurons against ongoing degeneration, such as glial cell line-derived neurotrophic factor; and genes encoding proteins that produce the inhibitory transmitter γ-aminobutylic acid (GABA) in the subthalamic nucleus (STN), thus suppressing the hyperactive STN. Recombinant adeno-associated viral (rAAV) vectors, which are derived from non-pathogenic viruses, have been shown to be suitable for clinical trials. These rAAVs have been found to transduce substantial numbers of neurons efficiently and to express transgenes in mammalian brains for long periods of time, with minimum inflammatory and immunological responses. *In vivo* imaging using positron emission tomography is useful for monitoring transgene expression and for assessing the functional effects of gene delivery. Vector systems that regulate transgene expression are necessary to increase safety in clinical applications, and the development of such systems is in progress.

Keywords: AAV, adeno-associated virus, dopamine, gene therapy, glial cell line-derived neurotrophic factor, Parkinson's disease, positron emission tomography

Expert Opin. Biol. Ther. (2005) 5(5):663-671

1. Introduction

Parkinson's disease (PD) is a common neurodegenerative disorder among the elderly, with an estimated prevalence of 1% in individuals > 60 years old. During the progression of PD there is a loss of neurons in the substantia nigra pars compacta (SNc), which projects to the striatum (caudate and putamen), leading to a substantial decrease in the dopamine (DA) content of the striatum. Although our understanding of the molecular basis of PD has advanced following the identification of mutations in the *α-synuclein*, *parkin*, *DJ-1*, *PINK1* and *LRRK2* genes associated with familial PD [1-3], the cause of PD largely remains unknown and to date there is no curative therapy.

The primary symptoms of PD are motor disturbances, including resting tremor, muscular rigidity and bradykinesia. These symptoms become apparent after 40 – 50% of the neurons in the SNc have been lost and striatal DA has been reduced to ~ 20% of normal levels [4]. The introduction of the DA precursor L-3,4-dihydroxyphenylalanine (L-dopa) in the late 1960s represented a major therapeutic advance in the management of PD, demonstrating that the replacement of DA is important in alleviating the motor symptoms of this disease. Although virtually all PD patients benefit clinically from L-dopa therapy, L-dopa becomes less effective as the disease progresses. Frequent systemic administration of high-dose L-dopa causes oscillations in motor performance [5,6] and deleterious

complications, including hallucinations due to dopaminergic stimulation of the mesolimbic system [7]. Thus, novel therapeutic interventions that complement or substitute for oral L-dopa administration are required.

Unlike other neurological disorders that affect broad regions of the brain, PD is primarily confined to the well-defined nigrostriatal dopaminergic system. Stereotactic techniques based on microelectrode recording of neural activities and magnetic resonance imaging-assisted navigation have become established in clinical practice and can be used in gene therapy to deliver vectors into the striatum.

2. Recombinant adeno-associated viral vectors

Among the various gene delivery vehicles tested preclinically for PD, the recombinant adeno-associated viral (rAAV) vector has been found most suitable for clinical applications, due to both its efficacy and safety. This vector is the only one based on the use of a non-pathogenic and replication-defective virus. Efficient and long-term gene expression has been achieved in mammalian brains without substantial toxicity or immune response [8-11]. Wild-type adeno-associated viruses (AAVs) are small, non-enveloped, single-stranded DNA viruses of the *Parvoviridae* family assigned to the genus *Dependovirus*. Productive infection with AAV has been found to require coinfection with a helper virus, such as adenovirus or herpes virus [12]. Until the mid-1990s, only AAV serotype 2 (AAV-2) had been sequenced, making it a major platform for gene therapy vector development [13-20]. So far > 100 different AAV sequences have been isolated from human and non-human primates [21], and their recombinants have been investigated extensively for tissue tropism and transduction efficiency. This has led to an increase in transduction efficiency, as well as being associated with changes in tissue or cell type tropism or vector distribution patterns in a given tissue [22-26].

Although chromosomal rearrangements in association with rAAV integration have been observed in a transformed cell line [27] and in regenerating hepatocytes [28], rAAV is more commonly present *in vivo* as duplex, circular and head-to-tail concatemers, most of which are episomal in non-dividing cells in the absence of selection [29]. Preferential integration into active regions of the chromosome and into actively transcribed genes is not unique to rAAV vectors [30], inasmuch as it has been noted even in adenoviruses, which are generally considered to be non-integrating. In addition, the promoter activity of the terminal repeat sequence of AAV is much weaker than that of retrovirus, probably limiting transcription to the inward direction of the viral genome. Thus, the risks of insertional mutagenesis and activation of oncogenes are quite low. Other safety aspects of rAAV vectors have been reviewed elsewhere [31,32].

Pre-existing antibodies to naturally infecting AAV-2 are found in 80% of the human population, and neutralising antibodies can be induced after rAAV vector administration. These antibodies may compromise transgene expression [33,34], and the presence of elevated neutralising antibody titres should be considered as exclusion criteria for clinical trials, although further studies are necessary to more specifically define the antibody titre that would constitute exclusion. Different rAAV vector serotypes will permit successful retransduction in response to significant levels of neutralising antibodies to one or more rAAV vectors.

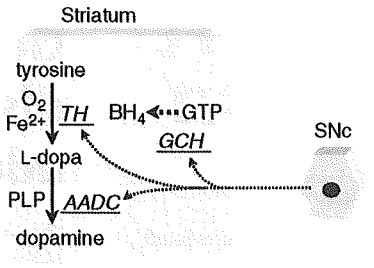

Figure 1. Biosynthetic pathway of DA. Three enzymes are necessary for efficient DA production. TH converts dietary tyrosine into L-dopa, which in turn is converted into DA by AADC. GCH is the rate-limiting enzyme for the biosynthesis of BH_4, the essential TH cofactor. All three of these enzymes are synthesised in the substantia nigra and transported to the striatum. Drastic reduction in the activities of these enzymes results in the depletion of DA in the striatum, leading to the manifestation of motor symptoms.
AADC: Aromatic-L-amino acid decarboxylase; BH_4: Tetrahydrobiopterin; DA: Dopamine; GCH: Guanosine triphosphate cyclohydrolase I; GTP: Guanosine triphosphate; L-dopa: L-3,4-dihydroxyphenylalanine; PLP: Pyridoxal 5'-phosphate; SNc: Substantia nigra pars compacta; TH: Tyrosine hydroxylase.

3. Local production of dopamine in the striatum

3.1 Biosynthesis of dopamine

One potential strategy of gene therapy for PD is to restore local production of DA by delivering genes of DA-synthesising enzymes into the striatum [9-11,35-39]. Three enzymes are necessary for efficient DA synthesis: tyrosine hydroxylase (TH), aromatic L-amino acid decarboxylase (AADC) and guanosine triphosphate cyclohydrolase I (GCH) (Figure 1). TH is the rate-limiting enzyme that converts L-tyrosine to L-dopa; AADC converts L-dopa to DA; and GCH is the rate-limiting enzyme in the biosynthesis of the essential TH cofactor, tetrahydrobiopterine (BH_4). These three enzymes are synthesised in SNc neurons and are anterogradely transported to the striatum. In advanced PD, the severe loss of dopaminergic nerve terminals is associated with an 80 – 95% depletion of striatal TH and AADC activity [40-42], leading to a profound decrease in DA. Failure to respond to L-dopa therapy may result from a reduction in AADC activity, decreased DA storage capacity in synaptic vesicles, postsynaptic changes in striatal output neurons and/or abnormalities of non-dopaminergic neurotransmitter systems. AADC is present in DA-denervated striatum within non-dopaminergic neurons and glial cells, but endogenous AADC activity in the

striatum is considered insufficient, at least in primates [35,43]. Although L-dopa may function as a neurotransmitter or modify behaviour through DA-independent mechanisms, central inhibition of AADC with 3-hydroxybenzylhydrazine (NSD-1015) has been shown to result in the abolition of the L-dopa motor effect [44], corroborating the classical concept that L-dopa is pharmacologically inert and its effects are mediated by DA and metabolites. Thus, most of the L-dopa produced in the striatum after gene transfer must be converted to DA *in situ*. Along with decreases in the levels of BH_4, TH and DA observed in PD, the activity of GCH in the striatum is also decreased in this disease [45]. As a low level of endogenous BH_4 does not yield sufficient TH activity, GCH is thought to regulate TH activity by regulating BH_4 biosynthesis, thus indirectly controlling DA production in TH-containing DA neurons [45-47]. In dominantly inherited dopa-responsive dystonia, a mutation in the gene encoding GCH results in a decrease in the level of BH_4, a further decrease in TH activity and a decrease in DA production [48]. Although BH_4 can cross the blood–brain barrier, uptake of exogenous BH_4 from the blood is low [49] and the primary source of BH_4 in the brain is via intracellular biosynthesis. Thus, GCH gene transfer into striatal cells may offer a more efficient method of supplying BH_4 than its exogenous administration.

3.2 Dopamine production in animal models

The availability of well-characterised rodent and non-human primate models makes PD a suitable candidate for gene therapy experiments. These models use neurotoxins that selectively elicit DA neuronal death in the SNc and deplete nigrostrital DA. A rat model of PD is generated by injecting 6-hydroxydopamine (6-OHDA) into the striatum or nigrostriatal pathway [50]. Systemic or intracarotid administration of 1-methyl-4-phenyl-1,2,3,6-tetrahydropyridine (MPTP) into monkeys replicates all the cardinal signs of PD, including tremor, rigidity, bradykinesia and postural instability. The primate MPTP model is useful in evaluating motor functions and in assaying transduction efficiency in the larger striatum.

The limited packaging capacity of rAAV vectors (< 5 kb) makes it impossible to use a single vector to express all three enzymes. However, one cell could be simultaneously transduced with multiple rAAV vectors encoding different enzymes. Although the addition of AADC via genetically modified fibroblasts to a system expressing TH and GCH has been reported to result in reduced production of L-dopa, due to feedback inhibition of DA on TH [51,52], direct gene transfer of AADC and TH into the striatum using rAAV vectors has been found to be beneficial in 6-OHDA-lesioned rats [10,36]. Local production of striatal DA was higher in cells expressing GCH, TH and AADC than in cells expressing TH and AADC, and these results have been confirmed in a primate model [38]. rAAV vectors have been shown to efficiently introduce genes encoding DA-synthesising enzymes into the striatum of the MPTP model, resulting in the restoration of motor functions with robust transgene expression and elevated DA synthesis in the treated putamen.

So far, dyskinesia has not been observed in preclinical studies of rAAV vector-mediated gene delivery of DA-synthesising enzymes. Moreover, rAAV vector-mediated delivery of TH and GCH was found to reverse peak-dose dyskinesia in a rat model of PD [53]. Continuous DA production in the striatum may account for the reduced likelihood of dyskinesia. It has been clinically shown that, compared with drugs that have a long duration of effect, short-acting pulsatile DA agonists are more likely to induce dyskinesia in PD patients [5]. Compared with conventional oral therapies, continuous intraduodenal infusion of L-dopa/carbidopa has a greater effect on motor performance improvement, but without increasing dyskinesia [54].

Gene transfer of AADC alone, in combination with oral administration of L-dopa, could be a shortcut to start clinical trials in PD patients [35,39]. Although these patients would still need to take L-dopa to control their PD symptoms, DA production could be regulated by altering the dose of L-dopa. It could be argued that the major reason for failure of L-dopa therapy is that adverse effects overwhelm the therapeutic response (shrinking of the therapeutic window). Many of the late-stage complications of PD result from the very high doses of L-dopa required to induce a therapeutic response. Experimental and clinical experience using inhibitors of catechol-*O*-methyl-transferase (COMT) indicates that a reduction in the dose of L-dopa is important in controlling the dyskinesia associated with prolonged DA half-life [55]. Restoring decarboxylating capacity by gene transfer could potentially allow lower doses of L-dopa and reduce the long-term adverse effects associated with escalating L-dopa therapy [10,35,39,41,56].

4. Protection of the nigrostriatal pathway

An alternative approach to the treatment of PD is to protect the nigrostriatal pathway from progressive degeneration by providing genes encoding growth factors [57], antioxidant molecules or antiapoptotic substances [58]. The slow progressive nature of degeneration in PD makes this approach attractive for arresting or even reversing parkinsonian symptoms. One potential candidate for this strategy is glial cell line-derived neurotrophic factor (GDNF) [57,59], a small glycoprotein that provides strong tropic support for DA neurons [60]. Application of the GDNF protein, however, is limited by its short half-life and its poor ability to cross the blood–brain barrier. An attempt to treat PD patients by direct injection of GDNF protein into the ventricles was unsuccessful [61]. A Phase I safety trial of continuous delivery of GDNF into the postero-dorsal putamen of five PD patients showed alleviation of off-medication motor symptoms and dyskinesia [62], and positron emission tomography (PET) detected increased DA storage, both in the putamen and the substantia nigra, suggesting retrograde transport of GDNF. Delivery of the gene encoding GDNF by viral vectors would be advantageous for PD patients, in that a single injection

would provide sustained GDNF production in the brain. This method does not require implantation of an infusion device, which is likely to increase patient morbidity as well as long-term risks of infection. Many studies have demonstrated that delivery of the *GDNF* gene via rAAV [63-67], adenoviral [68-73] or lentiviral [74,75] vectors protects nigral DA neurons in rodent and primate models of PD. Intrastriatal administration of rAAV vector expressing GDNF prevented the degeneration of DA neurons and promoted behavioural recovery, even 4 – 5 weeks after the onset of progressive degeneration [66,67]. This delayed rescue is important for clinical application, as a substantial number of DA neurons are lost prior to the appearance of symptoms characteristic of PD.

Striatal GDNF appears to be important for the occurrence of functional reinnervation. However, the expression of GDNF in nigral DA neurons may be detrimental, because intense local sprouting may prevent regeneration of the lesioned axons toward the striatum [64,76,77]. Expression of low levels of GDNF in the striatum is sufficient to provide protective effects without affecting DA synthesis [78]. Although it remains to be verified whether neurotoxin-induced animal models faithfully reflect the human disease, neuroprotective gene therapy with neurotrophic factors holds promise as a novel treatment of PD. Furthermore, neuroimaging techniques [79] and genetic analysis of some familial cases [1,3] have provided an opportunity for detecting at-risk individuals prior to the appearance of the symptoms characteristic of PD, thus enabling the application of earlier gene therapy with GDNF.

5. Suppression of the overactive subthalamic nucleus

Hyperactivity of the subthalamic nucleus (STN) is considered a major functional abnormality of PD [80]. Based on a model of basal ganglia circuitry, depletion of DA in the striatum increases the activity of neurons expressing the D2 receptor. These neurons send their inhibitory projections to the external segment of the globus pallidus (GPe), which leads to the over-inhibition of GPe neurons. Reduced inhibitory input from GPe in the STN results in overactivation of the nucleus, and excessive drive of the STN to the internal segment of the globus pallidus (GPi) and to the substantia nigra pars reticulata (SNr) exerts inhibitory effects on the thalamocortical projection and brainstem nucleus. During the past decade, deep brain stimulation of the STN, which may modify STN output, has become a routine treatment for advanced PD patients, providing improvements in motor function, although the fundamental mechanism of STN stimulation remains to be defined. The success of STN stimulation in PD patients, together with the symptomatic relief mimicked by infusion of the $GABA_A$ agonist into the STN [81] or directly into the SNr [82] in a primate model of PD, suggests another gene therapy approach: rAAV vector-mediated gene transfer of glutamate decarboxylase (GAD), an enzyme involved in the biosynthesis of the inhibitory neurotransmitter γ-aminobutylic acid (GABA), into the STN [83,84]. The underlining physiological changes in PD include, in addition to increases in the firing rate of the STN, the tendency of pallidal neurons to fire in more irregular patterns, as well as abnormal oscillatory synchronisation in the basal ganglia [85]. A Phase I clinical trial is underway at present to determine the extent to which *GAD* gene transfer into the STN remedies these abnormalities.

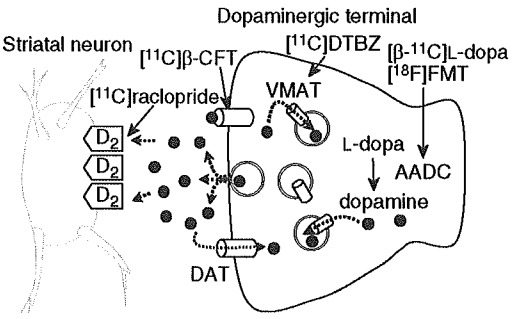

Figure 2. Schematic diagram of a DA synapse, demonstrating specific ligands for PET. [β-^{11}C]L-dopa and [^{18}F]FMT are AADC substrates. Transporter markers include high-affinity ligands for the neuronal DAT, including the cocaine analogue [^{11}C]β-CFT, as well as ligands that bind the VMAT2, such as [^{11}C]DTBZ. Ligands for the D_2 receptor, such as [^{11}C]raclopride, compete with DA and reflect the synaptic DA level. Black circles represent DA.
[β-^{11}C]L-dopa: [β-^{11}C]L-3,4-dihydroxyphenylalanine;
[^{11}C]β-CFT: [^{11}C]2β-carbomethoxy-3β-(4-fluorophenyl)tropane;
AADC: Aromatic-L-amino acid decarboxylase; DA: Dopamine;
DAT: DA transporter; [^{11}C]DTBZ: [^{11}C]dihydrotetrabenazine;
[^{18}F]FMT: 6-[^{18}F]-*m*-tyrosine; PET: Positron emission tomography;
VMAT: Vesicular monoamine transporter.

6. *In vivo* monitoring of transgenes by PET

PET is a valuable technique for imaging altered DA function in PD [86-88]. The effects of therapeutic gene delivery can be assessed using specific positron-labelled ligands developed for evaluating each process of DA turnover [89] (**Figure 2**). In addition, the level and duration of transgene expression can be directly monitored *in vivo* when the tracer is a substrate for the transgene product [90]. The first tracer used to visualise and assess the integrity of DA presynaptic systems was 6-[^{18}F]-fluoro-L-dopa (FDOPA), a fluoro-analogue of L-dopa. FDOPA is taken up into the DA terminals, decarboxylated by AADC, trapped and stored in synaptic vesicles. FDOPA uptake is highly correlated with viable DA cells in MPTP-lesioned monkeys [91] and in post-mortem human PD brains [92]. One shortcoming that complicates the use of this agent is that metabolites of FDOPA, such as 3-*O*-methyl–FDOPA, formed by the action of the ubiquitous enzyme COMT, enter the brain and diminish image contrast. An alternative tracer is [β-^{11}C]L-dopa, which undergoes less 3-*O*-methylation [93,94] and has a shorter half-life (20 min for ^{11}C). The use of this tracer has made it possible to obtain sequential imaging data not only

during the early steps of DA metabolism (e.g., decarboxylation by AADC), but also during DA receptor binding and DA transporter availability in the same subject on the same day. With an ~ 2-h interval between PET scans, each can be performed without any interference by radioactivity from the previous scan. In addition, PET scans can be performed using the non-catecholic tracer 6-[^{18}F]-*m*-tyrosine (FMT), which is also a good substrate for AADC and is not metabolised by COMT [87,90,95]. As FMT uptake has about twice the sensitivity of FDOPA uptake, FMT and [β-^{11}C]L-dopa are the ligands of choice for assessing the distribution and activity of AADC delivered by rAAV vectors.

To evaluate the functional effects of gene therapy in PD, DA release following pharmacological challenges can be measured indirectly *in vivo*, as reflected by reductions of DA receptor availability to selective antagonists such as [^{11}C]raclopride [96-98]. A 1% change in striatal [^{11}C]raclopride binding corresponds to at least an 8% change in synaptic DA levels [99]. PET measurements with [^{15}O]H_2O can also monitor alterations in regional cerebral blood flow, both during resting conditions and in response to stimuli. In PD, activation was found to be reduced in the premotor and prefrontal cortices during performance of a paced motor task [100].

7. Regulation of transgene expression

Most of the existing rAAV vectors rely on strong viral promoters that exhibit constitutive expression of transgenes. Excess production of therapeutic proteins, however, can often cause adverse effects. Vector constructs that allow the regulation of gene expression are necessary to maintain functional concentrations within therapeutic windows. However, so far there are no clinically available regulatable systems based on rAAV vectors, although several systems have been developed for preclinical studies. The most popular systems incorporate inducible promoters, which can respond to drugs and/or hormones. Inducing agents employed in these systems include RU486 (mefipristone) [101], rapamycin [102] and tetracycline [103]. Another system by which transgene expression can be shut down is viral vector-mediated delivery of bacteriophage Cre recombinase [104]. In this system, the therapeutic gene is flanked by *lox*P sequences, allowing the Cre recombinase to excise the transgene. RNA technology, including RNA interference [105,106] and ribozymes [107,108], has become more popular, and these systems can be used to reduce transgene expression. In addition, cell type-specific promoters may be useful for targeting specific brain regions, although rAAV vectors based on AAV2 preferentially transduce neurons.

8. Expert opinion and conclusion

rAAV vectors have been found to expand the potential of gene therapy, allowing the treatment of a wide range of neurological diseases, including PD [25,109]. Two Phase I clinical trials testing rAAV vectors for PD have been initiated in the US. These trials involve the delivery of the *GAD* gene into the STN and the delivery of the *AADC* gene into the putamen. Vectors used in these protocols do not contain a regulatory component for controlling gene expression. However, stimulation or coagulation of STN potentially reverses the unanticipated effects of GAD expression, and DA cannot be synthesised in the absence of L-dopa administration after transfer of the *AADC* gene. Incorporation of a regulatory component is necessary to increase safety in future clinical trials that are intended to allow local DA synthesis without L-dopa administration. However, DA receptor antagonists, such as haloperidol, could be used in cases of DA overproduction.

Fetal cell transplantation has been applied clinically to patients with advanced PD, with the intention of replacing the degenerated DA neurons. If the primary mechanism underlying recovery in these cell therapies is restoration of dopaminergic neurotransmission, a more straightforward approach would be direct delivery of genes encoding DA-synthesising enzymes into the striatum. However, replacement of DA in the striatum may have no effect on non-motor problems in PD, including affective and autonomic disturbances associated with pathologies not involving dopaminergic pathway degeneration. Broad regions of the brain beyond the motor parts of the basal ganglia are involved in the manifestation of L-dopa-induced dyskinesia [110]. This should be considered when delivery of the *TH* and *GCH* genes is intended to reduce dyskinesia. If reconstruction of the neural network, including the nigrostriatal pathway, is necessary to ameliorate the more complex symptoms of PD, such as dementia, a combination of gene therapy and cell transplantation would be the next strategy for overcoming this complex task. Ongoing clinical trials should provide information showing the extent to which rAAV-mediated gene therapy alleviates motor symptoms in advanced PD patients who responded to L-dopa therapy at early stages.

Recently developed neuroimaging techniques and genetic analysis in some familial cases of PD may provide information enabling the identification of at-risk individuals before characteristic symptoms appear. Earlier gene therapy with neuroprotective molecules could be applied to these at-risk individuals, as well as to patients known to have PD. The elucidation of the mechanism by which genetic mutations lead to the loss of DA neurons in familial forms of PD, as well as the detection of factors that increase the risk for PD, will provide new targets for gene therapy [111].

Bibliography

Papers of special note have been highlighted as either of interest (•) or of considerable interest (••) to readers.

▶1. HEALY DG, ABOU-SLEIMAN PM, WOOD NW: PINK, PANK, or PARK? A clinicians' guide to familial parkinsonism. *Lancet Neurol.* (2004) 3(11):652-662.

▶2. SHEN J: Protein kinases linked to the pathogenesis of Parkinson's disease. *Neuron* (2004) 44(4):575-577.

▶3. VILA M, PRZEDBORSKI S: Genetic clues to the pathogenesis of Parkinson's disease. *Nat. Med.* (2004) 10(Suppl.):S58-S62.

4. KISH SJ, SHANNAK K, HORNYKIEWICZ O: Uneven pattern of dopamine loss in the striatum of patients with idiopathic Parkinson's disease. Pathophysiologic and clinical implications. *N. Engl. J. Med.* (1988) 318(14):876-880.

5. JENNER P: Factors influencing the onset and persistence of dyskinesia in MPTP-treated primates. *Ann. Neurol.* (2000) 47(4 Suppl. 1):S90-S104.

6. LANGSTON JW, QUIK M, PETZINGER G, JAKOWEC M, DI MONTE DA: Investigating levodopa-induced dyskinesias in the parkinsonian primate. *Ann. Neurol.* (2000) 47(4 Suppl. 1):S79-S89.

▶7. CAREY RJ, PINHEIRO-CARRERA M, DAI H, TOMAZ C, HUSTON JP: L-DOPA and psychosis: evidence for L-DOPA-induced increases in prefrontal cortex dopamine and in serum corticosterone. *Biol. Psychiatry* (1995) 38(10):669-676.

8. DU B, WU P, BOLDT-HOULE DM, TERWILLIGER EF: Efficient transduction of human neurons with an adeno-associated virus vector. *Gene Ther.* (1996) 3(3):254-261.

▶9. KAPLITT MG, LEONE P, SAMULSKI RJ *et al.*: Long-term gene expression and phenotypic correction using adeno-associated virus vectors in the mammalian brain. *Nat. Genet.* (1994) 8(2):148-154.

• **First report of rAAV vector-mediated gene delivery in an animal model of PD.**

▶10. LEFF SE, SPRATT SK, SNYDER RO, MANDEL RJ: Long-term restoration of striatal L-aromatic amino acid decarboxylase activity using recombinant adeno-associated viral vector gene transfer in a rodent model of Parkinson's disease. *Neuroscience* (1999) 92(1):185-196.

• **One of a series of reports describing DA replacement using rAAV vectors.**

▶11. SHEN Y, MURAMATSU SI, IKEGUCHI K *et al.*: Triple transduction with adeno-associated virus vectors expressing tyrosine hydroxylase, aromatic-L-amino-acid decarboxylase, and GTP cyclohydrolase I for gene therapy of Parkinson's disease. *Hum. Gene Ther.* (2000) 11(11):1509-1519.

• **One of a series of reports describing DA replacement using rAAV vectors.**

12. BERNS KI, BERGOIN M, BLOOM M *et al.*: Family Parvoviridae. In: *Virus Taxonomy. Classification and Nomenclature of Viruses.* Murphy FA (Ed.), Springer-Verlag, New York, USA (1995):169-178.

13. BANTEL-SCHAAL U, DELIUS H, SCHMIDT R, ZUR HAUSEN H: Human adeno-associated virus type 5 is only distantly related to other known primate helper-dependent parvoviruses. *J. Virol.* (1999) 73(2):939-947.

14. CHIORINI JA, KIM F, YANG L, KOTIN RM: Cloning and characterization of adeno-associated virus type 5. *J. Virol.* (1999) 73(2):1309-1319.

15. CHIORINI JA, YANG L, LIU Y, SAFER B, KOTIN RM: Cloning of adeno-associated virus type 4 (AAV4) and generation of recombinant AAV4 particles. *J. Virol.* (1997) 71(9):6823-6833.

▶16. HANDA A, MURAMATSU S, QIU J, MIZUKAMI H, BROWN KE: Adeno-associated virus (AAV)-3-based vectors transduce haematopoietic cells not susceptible to transduction with AAV-2-based vectors. *J. Gen. Virol.* (2000) 81(Pt 8):2077-2084.

▶17. MURAMATSU S, MIZUKAMI H, YOUNG NS, BROWN KE: Nucleotide sequencing and generation of an infectious clone of adeno-associated virus 3. *Virology* (1996) 221(1):208-217.

18. RUTLEDGE EA, HALBERT CL, RUSSELL DW: Infectious clones and vectors derived from adeno-associated virus (AAV) serotypes other than AAV type 2. *J. Virol.* (1998) 72(1):309-319.

19. SRIVASTAVA A, LUSBY EW, BERNS KI: Nucleotide sequence and organization of the adeno-associated virus 2 genome. *J. Virol.* (1983) 45(2):555-564.

▶20. XIAO W, CHIRMULE N, BERTA SC *et al.*: Gene therapy vectors based on adeno-associated virus type 1. *J. Virol.* (1999) 73(5):3994-4003.

▶21. GAO G, VANDENBERGHE LH, ALVIRA MR *et al.*: Clades of adeno-associated viruses are widely disseminated in human tissues. *J. Virol.* (2004) 78(12):6381-6388.

• **Describes novel primate AAVs.**

▶22. BURGER C, GORBATYUK OS, VELARDO MJ *et al.*: Recombinant AAV viral vectors pseudotyped with viral capsids from serotypes 1, 2, and 5 display differential efficiency and cell tropism after delivery to different regions of the central nervous system. *Mol. Ther.* (2004) 10(2):302-317.

23. DAVIDSON BL, CHIORINI JA: Recombinant adeno-associated viral vector types 4 and 5. Preparation and application for CNS gene transfer. *Methods Mol. Med.* (2003) 76:269-285.

▶24. NAKAI H, FUESS S, STORM TA *et al.*: Unrestricted hepatocyte transduction with adeno-associated virus serotype 8 vectors in mice. *J. Virol.* (2005) 79(1):214-224.

▶25. TENENBAUM L, CHTARTO A, LEHTONEN E *et al.*: Recombinant AAV-mediated gene delivery to the central nervous system. *J. Gene Med.* (2004) 6(Suppl. 1):S212-S222.

▶26. WANG C, WANG CM, CLARK KR, SFERRA TJ: Recombinant AAV serotype 1 transduction efficiency and tropism in the murine brain. *Gene Ther.* (2003) 10(17):1528-1534.

▶27. MILLER DG, RUTLEDGE EA, RUSSELL DW: Chromosomal effects of adeno-associated virus vector integration. *Nat. Genet.* (2002) 30(2):147-148.

▶28. NAKAI H, MONTINI E, FUESS S *et al.*: AAV serotype 2 vectors preferentially integrate into active genes in mice. *Nat. Genet.* (2003) 34(3):297-302.

▶29. SCHNEPP BC, CLARK KR, KLEMANSKI DL, PACAK CA, JOHNSON PR: Genetic fate of recombinant adeno-associated virus vector genomes in muscle. *J. Virol.* (2003) 77(6):3495-3504.

▶30. MCCARTY DM, YOUNG SM JR, SAMULSKI RJ: Integration of adeno-associated virus (AAV) and recombinant AAV vectors. *Annu. Rev. Genet.* (2004) 38:819-845.

▶31. MONAHAN PE, JOOSS K, SANDS MS: Safety of adeno-associated virus gene therapy vectors: a current evaluation. *Expert Opin. Drug Saf.* (2002) 1(1):79-91.

• **A review on the safety aspects of rAAV vectors.**

32. TENENBAUM L, LEHTONEN E, MONAHAN PE: Evaluation of risks related to the use of adeno-associated virus-based vectors. *Curr. Gene Ther.* (2003) 3(6):545-565.
- **A review on the safety aspects of rAAV vectors.**

▶33. PEDEN CS, BURGER C, MUZYCZKA N, MANDEL RJ: Circulating anti-wild-type adeno-associated virus type 2 (AAV2) antibodies inhibit recombinant AAV2 (rAAV2)-mediated, but not rAAV5-mediated, gene transfer in the brain. *J. Virol.* (2004) 78(12):6344-6359.

▶34. SANFTNER LM, SUZUKI BM, DOROUDCHI MM *et al.*: Striatal delivery of rAAV-hAADC to rats with preexisting immunity to AAV. *Mol. Ther.* (2004) 9(3):403-409.

▶35. BANKIEWICZ KS, EBERLING JL, KOHUTNICKA M *et al.*: Convection-enhanced delivery of AAV vector in parkinsonian monkeys; *in vivo* detection of gene expression and restoration of dopaminergic function using pro-drug approach. *Exp. Neurol.* (2000) 164(1):2-14.
- •• **rAAV vector-mediated *AADC* gene transfer in a primate model of PD.**

▶36. FAN DS, OGAWA M, FUJIMOTO KI *et al.*: Behavioral recovery in 6-hydroxydopamine-lesioned rats by cotransduction of striatum with tyrosine hydroxylase and aromatic L- amino acid decarboxylase genes using two separate adeno-associated virus vectors. *Hum. Gene Ther.* (1998) 9(17):2527-2535.

▶37. MANDEL RJ, RENDAHL KG, SPRATT SK *et al.*: Characterization of intrastriatal recombinant adeno-associated virus-mediated gene transfer of human tyrosine hydroxylase and human GTP-cyclohydrolase I in a rat model of Parkinson's disease. *J. Neurosci.* (1998) 18(11):4271-4284.
- **One of a series of reports describing DA replacement using rAAV vectors.**

▶38. MURAMATSU S, FUJIMOTO K, IKEGUCHI K *et al.*: Behavioral recovery in a primate model of Parkinson's disease by triple transduction of striatal cells with adeno-associated viral vectors expressing dopamine-synthesizing enzymes. *Hum. Gene Ther.* (2002) 13(3):345-354.
- •• **Demonstrates behavioural improvement in a primate model of PD.**

▶39. SANCHEZ-PERNAUTE R, HARVEY-WHITE J, CUNNINGHAM J, BANKIEWICZ KS: Functional effect of adeno-associated virus mediated gene transfer of aromatic L-amino acid decarboxylase into the striatum of 6-OHDA-lesioned rats. *Mol. Ther.* (2001) 4(4):324-330.
- **One of a series of reports describing DA replacement using rAAV vectors.**

40. ICHINOSE H, OHYE T, FUJITA K *et al.*: Quantification of mRNA of tyrosine hydroxylase and aromatic L-amino acid decarboxylase in the substantia nigra in Parkinson's disease and schizophrenia. *J. Neural Transm. Park. Dis. Dement. Sect.* (1994) 8(1-2):149-158.

41. KADDIS FG, CLARKSON ED, WEBER MJ *et al.*: Intrastriatal grafting of Cos cells stably expressing human aromatic L-amino acid decarboxylase: neurochemical effects. *J. Neurochem.* (1997) 68(4):1520-1526.

42. ZHONG XH, HAYCOCK JW, SHANNAK K *et al.*: Striatal dihydroxyphenylalanine decarboxylase and tyrosine hydroxylase protein in idiopathic Parkinson's disease and dominantly inherited olivopontocerebellar atrophy. *Mov. Disord.* (1995) 10(1):10-17.

43. NAKAMURA K, AHMED M, BARR E, LEIDEN JM, KANG UJ: The localization and functional contribution of striatal aromatic L-amino acid decarboxylase to L-3,4-dihydroxyphenylalanine decarboxylation in rodent parkinsonian models. *Cell Transplant.* (2000) 9(5):567-576.

▶44. TRESEDER SA, JACKSON M, JENNER P: The effects of central aromatic amino acid DOPA decarboxylase inhibition on the motor actions of L-DOPA and dopamine agonists in MPTP-treated primates. *Br. J. Pharmacol.* (2000) 129(7):1355-1364.

▶45. NAGATSU T, ICHINOSE H: Molecular biology of catecholamine-related enzymes in relation to Parkinson's disease. *Cell. Mol. Neurobiol.* (1999) 19(1):57-66.

▶46. CORTI O, SANCHEZ-CAPELO A, COLIN P *et al.*: Long-term doxycycline-controlled expression of human tyrosine hydroxylase after direct adenovirus-mediated gene transfer to a rat model of Parkinson's disease. *Proc. Natl. Acad. Sci. USA* (1999) 96(21):12120-12125.

▶47. NAGATSU T, HORIKOSHI T, SAWADA M *et al.*: Biosynthesis of tetrahydrobiopterin in parkinsonian human brain. *Adv. Neurol.* (1987) 45:223-226.

▶48. ICHINOSE H, OHYE T, TAKAHASHI E *et al.*: Hereditary progressive dystonia with marked diurnal fluctuation caused by mutations in the GTP cyclohydrolase I gene. *Nat. Genet.* (1994) 8(3):236-242.

49. HOSHIGA M, HATAKEYAMA K, WATANABE M, SHIMADA M, KAGAMIYAMA H: Autoradiographic distribution of [14C]tetrahydrobiopterin and its developmental change in mice. *J. Pharmacol. Exp. Ther.* (1993) 267(2):971-978.

▶50. DEUMENS R, BLOKLAND A, PRICKAERTS J: Modeling Parkinson's disease in rats: an evaluation of 6-OHDA lesions of the nigrostriatal pathway. *Exp. Neurol.* (2002) 175(2):303-317.

▶51. KANG UJ, LEE WY, CHANG JW: Gene therapy for Parkinson's disease: determining the genes necessary for optimal dopamine replacement in rat models. *Hum. Cell* (2001) 14(1):39-48.

▶52. WACHTEL SR, BENCSICS C, KANG UJ: Role of aromatic L-amino acid decarboxylase for dopamine replacement by genetically modified fibroblasts in a rat model of Parkinson's disease. *J. Neurochem.* (1997) 69(5):2055-2063.

▶53. CARLSSON T, WINKLER C, BURGER C *et al.*: Reversal of dyskinesias in an animal model of Parkinson's disease by continuous L-DOPA delivery using rAAV vectors. *Brain* (2005) 128(Pt 3):559-569.

54. NYHOLM D, NILSSON REMAHL AI, DIZDAR N *et al.*: Duodenal levodopa infusion monotherapy versus oral polypharmacy in advanced Parkinson's disease. *Neurology* (2005) 64(2):216-223.

55. OLANOW CW, WATTS RL, KOLLER WC: An algorithm (decision tree) for the management of Parkinson's disease (2001): treatment guidelines. *Neurology* (2001) 56(11 Suppl. 5):S1-S88.

▶56. KIRIK D, GEORGIEVSKA B, BURGER C *et al.*: Reversal of motor impairments in parkinsonian rats by continuous intrastriatal delivery of L-dopa using rAAV-mediated gene transfer. *Proc. Natl. Acad. Sci. USA* (2002) 99(7):4708-4713.
- **One of a series of reports describing *GDNF* gene transfer using rAAV vectors in a rat model of PD.**

▶57. HURELBRINK CB, BARKER RA: The potential of GDNF as a treatment for Parkinson's disease. *Exp. Neurol.* (2004) 185(1):1-6.

▶ 58. MOCHIZUKI H, HAYAKAWA H, MIGITA M *et al.*: An AAV-derived Apaf-1 dominant negative inhibitor prevents MPTP toxicity as antiapoptotic gene therapy for Parkinson's disease. *Proc. Natl. Acad. Sci. USA* (2001) 98(19):10918-10923.

▶ 59. BOHN MC: Parkinson's disease: a neurodegenerative disease particularly amenable to gene therapy. *Mol. Ther.* (2000) 1(6):494-496.

▶ 60. LIN LF, DOHERTY DH, LILE JD, BEKTESH S, COLLINS F: GDNF: a glial cell line-derived neurotrophic factor for midbrain dopaminergic neurons. *Science* (1993) 260(5111):1130-1132.

▶ 61. KORDOWER JH, PALFI S, CHEN EY *et al.*: Clinicopathological findings following intraventricular glial-derived neurotrophic factor treatment in a patient with Parkinson's disease. *Ann. Neurol.* (1999) 46(3):419-424.

▶ 62. GILL SS, PATEL NK, HOTTON GR *et al.*: Direct brain infusion of glial cell line-derived neurotrophic factor in Parkinson's disease. *Nat. Med.* (2003) 9(5):589-595.

▶ 63. KIRIK D, ROSENBLAD C, BJORKLUND A, MANDEL RJ: Long-term rAAV-mediated gene transfer of GDNF in the rat Parkinson's model: intrastriatal but not intranigral transduction promotes functional regeneration in the lesioned nigrostriatal system. *J. Neurosci.* (2000) 20(12):4686-4700.

▶ 64. MANDEL RJ, SNYDER RO, LEFF SE: Recombinant adeno-associated viral vector-mediated glial cell line-derived neurotrophic factor gene transfer protects nigral dopamine neurons after onset of progressive degeneration in a rat model of Parkinson's disease. *Exp. Neurol.* (1999) 160(1):205-214.

▶ 65. MANDEL RJ, SPRATT SK, SNYDER RO, LEFF SE: Midbrain injection of recombinant adeno-associated virus encoding rat glial cell line-derived neurotrophic factor protects nigral neurons in a progressive 6-hydroxydopamine-induced degeneration model of Parkinson's disease in rats. *Proc. Natl. Acad. Sci. USA* (1997) 94(25):14083-14088.

66. MCGRATH J, LINTZ E, HOFFER BJ *et al.*: Adeno-associated viral delivery of GDNF promotes recovery of dopaminergic phenotype following a unilateral 6-hydroxydopamine lesion. *Cell Transplant.* (2002) 11(3):215-227.

▶ 67. WANG L, MURAMATSU S, LU Y *et al.*: Delayed delivery of AAV-GDNF prevents nigral neurodegeneration and promotes functional recovery in a rat model of Parkinson's disease. *Gene Ther.* (2002) 9(6):381-389.

▶ 68. BILANG-BLEUEL A, REVAH F, COLIN P *et al.*: Intrastriatal injection of an adenoviral vector expressing glial-cell-line-derived neurotrophic factor prevents dopaminergic neuron degeneration and behavioral impairment in a rat model of Parkinson's disease. *Proc. Natl. Acad. Sci. USA* (1997) 94(16):8818-8823.

▶ 69. CHOI-LUNDBERG DL, LIN Q, CHANG YN *et al.*: Dopaminergic neurons protected from degeneration by GDNF gene therapy. *Science* (1997) 275(5301):838-841.

▶ 70. CHOI-LUNDBERG DL, LIN Q, SCHALLERT T *et al.*: Behavioral and cellular protection of rat dopaminergic neurons by an adenoviral vector encoding glial cell line-derived neurotrophic factor. *Exp. Neurol.* (1998) 154(2):261-275.

▶ 71. CONNOR B, KOZLOWSKI DA, SCHALLERT T *et al.*: Differential effects of glial cell line-derived neurotrophic factor (GDNF) in the striatum and substantia nigra of the aged Parkinsonian rat. *Gene Ther.* (1999) 6(12):1936-1951.

▶ 72. CONNOR B, KOZLOWSKI DA, UNNERSTALL JR *et al.*: Glial cell line-derived neurotrophic factor (GDNF) gene delivery protects dopaminergic terminals from degeneration. *Exp. Neurol.* (2001) 169(1):83-95.

▶ 73. KOZLOWSKI DA, CONNOR B, TILLERSON JL, SCHALLERT T, BOHN MC: Delivery of a GDNF gene into the substantia nigra after a progressive 6- OHDA lesion maintains functional nigrostriatal connections. *Exp. Neurol.* (2000) 166(1):1-15.

▶ 74. AZZOUZ M, RALPH S, WONG LF *et al.*: Neuroprotection in a rat Parkinson model by GDNF gene therapy using EIAV vector. *Neuroreport* (2004) 15(6):985-990.

▶ 75. KORDOWER JH, EMBORG ME, BLOCH J *et al.*: Neurodegeneration prevented by lentiviral vector delivery of GDNF in primate models of Parkinson's disease. *Science* (2000) 290(5492):767-773.

•• ***GDNF* gene transfer using a lentiviral vector in a primate model of PD.**

76. GRONDIN R, GASH DM: Glial cell line-derived neurotrophic factor (GDNF): a drug candidate for the treatment of Parkinson's disease. *J. Neurol.* (1998) 245(11 Suppl. 3):P35-P42.

77. WALTON KM: GDNF: a novel factor with therapeutic potential for neurodegenerative disorders. *Mol. Neurobiol.* (1999) 19(1):43-59.

▶ 78. ESLAMBOLI A, GEORGIEVSKA B, RIDLEY RM *et al.*: Continuous low-level glial cell line-derived neurotrophic factor delivery using recombinant adeno-associated viral vectors provides neuroprotection and induces behavioral recovery in a primate model of Parkinson's disease. *J. Neurosci.* (2005) 25(4):769-777.

79. BROOKS DJ: Morphological and functional imaging studies on the diagnosis and progression of Parkinson's disease. *J. Neurol.* (2000) 247(Suppl. 2):II11- II18.

▶ 80. HAMANI C, SAINT-CYR JA, FRASER J, KAPLITT M, LOZANO AM: The subthalamic nucleus in the context of movement disorders. *Brain* (2004) 127(Pt 1):4-20.

▶ 81. LEVY R, LANG AE, DOSTROVSKY JO *et al.*: Lidocaine and muscimol microinjections in subthalamic nucleus reverse Parkinsonian symptoms. *Brain* (2001) 124(Pt 10):2105-2118.

▶ 82. WICHMANN T, KLIEM MA, DELONG MR: Antiparkinsonian and behavioral effects of inactivation of the substantia nigra pars reticulata in hemiparkinsonian primates. *Exp. Neurol.* (2001) 167(2):410-424.

83. DURING MJ, KAPLITT MG, STERN MB, EIDELBERG D: Subthalamic GAD gene transfer in Parkinson's disease patients who are candidates for deep brain stimulation. *Hum. Gene Ther.* (2001) 12(12):1589-1591.

▶ 84. LUO J, KAPLITT MG, FITZSIMONS HL *et al.*: Subthalamic GAD gene therapy in a Parkinson's disease rat model. *Science* (2002) 298(5592):425-429.

•• ***GAD* gene transfer into the STN using rAAV vectors.**

▶ 85. DOSTROVSKY J, BERGMAN H: Oscillatory activity in the basal ganglia-relationship to normal physiology and pathophysiology. *Brain* (2004) 127(Pt 4):721-722.

86. BROOKS DJ: PET studies on the function of dopamine in health and Parkinson's disease. *Ann. NY Acad. Sci.* (2003) 991:22-35.

• **A review on PET in PD.**

87. DOUDET DJ: PET studies in the MPTP model of Parkinson's disease. *Adv. Neurol.* (2001) 86:187-195.
• **A review on PET in a primate model of PD.**
88. RAVINA B, EIDELBERG D, AHLSKOG JE *et al.*: The role of radiotracer imaging in Parkinson's disease. *Neurology* (2005) 64(2):208-215.
89. DEJESUS OT: Positron-labeled DOPA analogs to image dopamine terminals. *Drug Dev. Res.* (2003) (59):249-260.
▶90. EBERLING JL, CUNNINGHAM J, PIVIROTTO P *et al.*: *In vivo* PET imaging of gene expression in Parkinsonian monkeys. *Mol. Ther.* (2003) 8(6):873-875.
▶91. PATE BD, KAWAMATA T, YAMADA T *et al.*: Correlation of striatal fluorodopa uptake in the MPTP monkey with dopaminergic indices. *Ann. Neurol.* (1993) 34(3):331-338.
▶92. SNOW BJ, TOOYAMA I, MCGEER EG *et al.*: Human positron emission tomographic [18F]fluorodopa studies correlate with dopamine cell counts and levels. *Ann. Neurol.* (1993) 34(3):324-330.
▶93. TORSTENSON R, TEDROFF J, HARTVIG P, FASTH KJ, LANGSTROM B: A comparison of 11C-labeled L-DOPA and L-fluorodopa as positron emission tomography tracers for the presynaptic dopaminergic system. *J. Cereb. Blood Flow Metab.* (1999) 19(10):1142-1149.
▶94. TSUKADA H, LINDNER KJ, HARTVIG P *et al.*: Effect of 6R-L-erythro-5,6,7,8-tetrahydrobiopterin and infusion of L-tyrosine on the *in vivo* L-[beta-11C] DOPA disposition in the monkey brain. *Brain Res.* (1996) 713(1-2):92-98.
95. HAYASE N, TOMIYOSHI K, WATANABE K *et al.*: Positron emission tomography with 4-[18F]fluoro-L-m-tyrosine in MPTP-induced hemiparkinsonian monkeys. *Ann. Nucl. Med.* (1995) 9(3):119-123.
96. TSUKADA H, HARADA N, NISHIYAMA S, OHBA H, KAKIUCHI T: Cholinergic neuronal modulation alters dopamine D2 receptor availability *in vivo* by regulating receptor affinity induced by facilitated synaptic dopamine turnover: positron emission tomography studies with microdialysis in the conscious monkey brain. *J. Neurosci.* (2000) 20(18):7067-7073.
▶97. TSUKADA H, HARADA N, NISHIYAMA S *et al.*: Ketamine decreased striatal [(11)C]raclopride binding with no alterations in static dopamine concentrations in the striatal extracellular fluid in the monkey brain: multiparametric PET studies combined with microdialysis analysis. *Synapse* (2000) 37(2):95-103.
▶98. TSUKADA H, NISHIYAMA S, KAKIUCHI T *et al.*: Is synaptic dopamine concentration the exclusive factor which alters the *in vivo* binding of [11C]raclopride? PET studies combined with microdialysis in conscious monkeys. *Brain Res.* (1999) 841(1-2):160-169.
▶99. BREIER A, SU TP, SAUNDERS R *et al.*: Schizophrenia is associated with elevated amphetamine-induced synaptic dopamine concentrations: evidence from a novel positron emission tomography method. *Proc. Natl. Acad. Sci. USA* (1997) 94(6):2569-2574.
▶100. BROOKS DJ: Functional imaging studies on dopamine and motor control. *J. Neural Transm.* (2001) 108(11):1283-1298.
▶101. NORDSTROM JL: The antiprogestin-dependent GeneSwitch system for regulated gene therapy. *Steroids* (2003) 68(10-13):1085-1094.
▶102. RIVERA VM, GAO GP, GRANT RL *et al.*: Long-term pharmacologically regulated expression of erythropoietin in primates following AAV-mediated gene transfer. *Blood* (2005) 105(4):1424-1430.
▶103. AGHA-MOHAMMADI S, O'MALLEY M, ETEMAD A *et al.*: Second-generation tetracycline-regulatable promoter: repositioned tet operator elements optimize transactivator synergy while shorter minimal promoter offers tight basal leakiness. *J. Gene Med.* (2004) 6(7):817-828.
▶104. AHMED BY, CHAKRAVARTHY S, EGGERS R *et al.*: Efficient delivery of Cre-recombinase to neurons *in vivo* and stable transduction of neurons using adeno-associated and lentiviral vectors. *BMC Neurosci.* (2004) 5(1):4.
▶105. CAPLEN NJ: Gene therapy progress and prospects. Downregulating gene expression: the impact of RNA interference. *Gene Ther.* (2004) 11(16):1241-1248.
106. WADHWA R, KAUL SC, MIYAGISHI M, TAIRA K: Vectors for RNA interference. *Curr. Opin. Mol. Ther.* (2004) 6(4):367-372.
▶107. WINKLER WC, NAHVI A, ROTH A, COLLINS JA, BREAKER RR: Control of gene expression by a natural metabolite-responsive ribozyme. *Nature* (2004) 428(6980):281-286.
▶108. YEN L, SVENDSEN J, LEE JS *et al.*: Exogenous control of mammalian gene expression through modulation of RNA self-cleavage. *Nature* (2004) 431(7007):471-476.
▶109. MURAMATSU S, WANG L, IKEGUCHI K *et al.*: Adeno-associated viral vectors for Parkinson's disease. *Int. Rev. Neurobiol.* (2003) 55:205-222.
▶110. GUIGONI C, LI Q, AUBERT I *et al.*: Involvement of sensorimotor, limbic, and associative basal ganglia domains in L-3,4-dihydroxyphenylalanine-induced dyskinesia. *J. Neurosci.* (2005) 25(8):2102-2107.
▶111. LO BIANCO C, SCHNEIDER BL, BAUER M *et al.*: Lentiviral vector delivery of parkin prevents dopaminergic degeneration in an alpha-synuclein rat model of Parkinson's disease. *Proc. Natl. Acad. Sci. USA* (2004) 101(50):17510-17515.

Affiliation

Shin-ichi Muramatsu[1†], Hideo Tsukada[2], Imaharu Nakano[1] & Keiya Ozawa[3]
†Author for correspondence
[1]Jichi Medical School, Division of Neurology, Department of Medicine, 3311-1 Yakushiji, Minami-kawachi, Tochigi, 3290498 Japan
Tel: +81 285 58 7352; Fax: +81 285 44 5118; E-mail: muramats@jichi.ac.jp
[2]Hamamatsu Photonics K.K., Central Research Laboratory, 5000 Hirakuchi, Hamakita, Shizuoka 434-8601, Japan
[3]Jichi Medical School, Division of Genetic Therapeutics, Center for Molecular Medicine, 3311-1 Yakushiji, Minami-kawachi, Tochigi, 3290498 Japan
Tel: +81 285 58 7402; Fax: +81 285 44 8675; E-mail: kozawa@jichi.ac.jp

Cerebrospinal Fluid Neprilysin is Reduced in Prodromal Alzheimer's Disease

Masahiro Maruyama, MD, PhD,[1] Makoto Higuchi, MD, PhD,[1,2] Yoshie Takaki, PhD,[2] Yukio Matsuba, BS,[2] Haruko Tanji, MD, PhD,[1] Miyako Nemoto, MD,[1] Naoki Tomita, MD,[1] Toshifumi Matsui, MD, PhD,[1] Nobuhisa Iwata, PhD,[2] Hiroaki Mizukami, MD, PhD,[3] Shin-ichi Muramatsu, MD, PhD,[3] Keiya Ozawa, MD, PhD,[3] Takaomi C. Saido, PhD,[2] Hiroyuki Arai, MD, PhD,[1] and Hidetada Sasaki, MD, PhD[1]

Amyloid β peptide (Aβ) has been implicated in Alzheimer's disease (AD) as an initiator of the pathological cascades. Several lines of compelling evidence have supported major roles of Aβ-degrading enzyme neprilysin in the pathogenesis of sporadic AD. Here, we have shown a substantial reduction of cerebrospinal fluid (CSF) neprilysin activity (CSF-NEP) in patients with AD-converted mild cognitive impairment and early AD as compared with age-matched control subjects. The altered CSF-NEP likely reflects changes in neuronal neprilysin, since transfer of neprilysin from brain tissue into CSF was demonstrated by injecting neprilysin-carrying viral vector into the brains of neprilysin-deficient mice. Interestingly, CSF-NEP showed an elevation with the progression of AD. Along with a close association of CSF-NEP with CSF tau proteins, this finding suggests that presynaptically located neprilysin can be released into CSF as a consequence of synaptic disruption. The impact of neuronal damages on CSF-NEP was further demonstrated by a prominent increase of CSF-NEP in rats exhibiting kainate-induced neurodegeneration. Our results unequivocally indicate significance of CSF-NEP as a biochemical indicator to pursue a pathological process that involves decreased neprilysin activity and Aβ-induced synaptic toxicity, and the support the potential benefits of neprilysin up-regulation in ameliorating neuropathology in prodromal and early AD.

Ann Neurol 2005;57:832–842

Numerous investigations have supported the contention that senile plaques and neurofibrillary lesions, composed primarily of amyloid β peptide (Aβ) and tau proteins, respectively, are not only descriptive characteristics of histopathology in brains with Alzheimer's disease (AD), but also mechanistically related to the pathogenesis of AD. That all of the genetic mutations causally linked to familial AD induce overproduction of either total Aβ or relatively amyloidogenic Aβ42[1] further provides supportive evidence for the role of Aβ accumulation as an initiator of the pathological cascade toward the onset of AD.[2]

The diagnosis of AD is definite based on magnitudes of these hallmark lesions after an autopsy, whereas exploitation of AD-specific biochemical markers reflecting central pathogenic processes, such as degeneration of neurites and synapses and alterations of Aβ and tau, for antemortem diagnosis is still ongoing. Since 1995, two categories of cerebrospinal fluid (CSF) markers, CSF-tau and CSF-Aβ42, have emerged and have proved to be useful indicators to assist clinical diagnosis of AD in living patients.[3–5] Furthermore, several recent studies have demonstrated usefulness of CSF-tau in differentiation of prodromal AD from AD-unrelated cognitive decline among patients with mild cognitive impairment (MCI).[6,7] In contrast, altered processing of amyloid precursor protein and Aβ has not been detected by biochemical markers such as CSF-Aβ42 in MCI patients,[6] although it is conceived to be upstream of tau abnormalities in the cascade of AD pathogenesis. Because therapeutic approaches, including existing drugs[8] and emerging treatments modifying Aβ pathology,[9,10] presumably have the greatest potential of being effective in the predementia phase of AD, accurate prediction of conversion to AD in patients with MCI by means of biological indices representing abnormal metabolism of amyloid precursor protein/Aβ is particularly crucial. This gives us a rationale of analyzing accessible body fluid in search for altered levels of

From the [1]Department of Geriatric Medicine, Tohoku University School of Medicine, Sendai, Miyagi; [2]Laboratory for Proteolytic Neuroscience, RIKEN Brain Science Institute, Wako, Saitama; and [3]Division of Genetic Therapeutics, Center for Molecular Medicine, Jichi Medical School, Minamikawachi, Tochigi, Japan.

Received Oct 22, 2004, and in revised form Feb 23, 2005. Accepted for publication Mar 14, 2005.

Published online May 23, 2005 in Wiley InterScience (www.interscience.wiley.com). DOI: 10.1002/ana.20494

Address correspondence to Dr Higuchi, Laboratory for Proteolytic Neuroscience, RIKEN Brain Science Institute, 2-1 Hirosawa, Wako, Saitama 351-0198, Japan. E-mail: mhiguchi@brain.riken.jp

Table 1. Clinical Characteristics of Study Subjects (mean ± SE)

Characteristic	Control	sMCI	pMCI	AD
No. of patients	27	5	33	32
Male/female ratio	7/19	5/0	10/13	9/23
Age (yr)	70.0 ± 1.5	74.4 ± 6.1	74.5 ± 1.0	73.1 ± 1.3
Years of education	10.8 ± 0.4	9.2 ± 0.1	11.7 ± 0.5	9.8 ± 0.9
MMSE score at baseline	28.6 ± 0.3	26.8 ± 0.8	25.3 ± 0.3	16.8 ± 1.0
Delayed recall score on WMS-R	95.0 ± 5.5	66.0 ± 4.3	58.5 ± 2.0	—
Years of follow-up	1.9 ± 0.1	1.9 ± 0.2	2.0 ± 0.4	1.3 ± 0.1
Changes in MMSE score by the end of follow-up	0.3 ± 0.1	−0.7 ± 0.3	−3.3 ± 0.4	−1.7 ± 0.6
Annual changes in MMSE score	0.14 ± 0.07	−0.39 ± 0.14	−1.74 ± 0.23	−1.48 ± 0.52

SE = standard error; sMCI = stable mild cognitive impairment; pMCI = progressive MCI; AD = Alzheimer's disease; MMSE = Mini-Mental State Examination; WMS-R = Wechsler Memory Scale–Revised.

molecules in close association with pathogenic Aβ accumulation in the brain.

One notable feature of Aβ metabolism is that it is a normal physiological process occurring in diverse cell types. Because there has been no overt evidence for an increased production of Aβ in sporadic AD, the molecular mechanism of Aβ degradation is of growing interest. The neutral endopeptidase neprilysin (EC 3.4.24.11) is one of the enzymes implicated in physiological Aβ catabolism.[11,12] In neurons, it is localized primarily to the presynaptic terminals, with its ectodomain facing extracellular matrix,[11,13] and thus is capable of degrading extracellular Aβ released from nerve ends. Recent genetic approaches using neprilysin-deficient mice have demonstrated the ability of neprilysin to cleave endogenous Aβ.[12,14] Moreover, a decline of neprilysin levels has also been found in the brains of patients with early-stage sporadic AD,[15] suggesting critical roles played by reduced neprilysin activity in the incipient process of Aβ accumulation.

The purpose of the study reported here was to assess applicability of monitoring neprilysin activities in CSF (CSF-NEP) and plasma (plasma-NEP) of patients with MCI and AD for prediction of clinical course and for gaining insights into molecular events early in Aβ pathogenesis. The results showed a significant decrease of CSF-NEP, which developed to AD, in patients with MCI and in patients with mild AD, indicating usefulness of CSF-NEP assay as an informative clinical adjunct.

Subjects and Methods

Subjects

We studied 96 patients (mean age ± standard error, 72.5 ± 0.8 years) who underwent evaluations for memory disturbance at the Tohoku University Hospital Outpatient Clinic on Dementia. Clinical assessments by geriatricians and neuropsychological examinations, including Mini-Mental State Examination (MMSE) and Wechsler Memory Scale–Revised were performed for all patients, as described in detail previously.[16] Our established criteria[16] based on the current consensus[17] were used for diagnosis of amnestic MCI, and a diagnosis of AD was made in accordance with the National Institute of Neurological and Communication Disorders-Alzheimer's Disease and Related Disorders Association criteria.[18] Consequently, 38 patients fulfilled the diagnostic criteria for amnestic MCI, 32 patients were diagnosed as having AD, and 26 patients were found to be cognitively normal at baseline investigation.

During the 2-year follow-up period, 33 of the patients with amnestic MCI progressed to AD and were thus classified into progressive MCI (pMCI). Five patients with amnestic MCI who showed unchanged or improved cognitive functions remained, and they were categorized as having stable MCI (sMCI). Twenty-eight patients with pMCI and all of the patients who were diagnosed as having AD at baseline were treated with a 5mg daily dose of donepezil hydrochloride.

At baseline examination, plasma and CSF samples were collected from each patient. CSF-tau was determined using a sandwich enzyme-linked immunosorbent assay designed for measurement of total tau (INNOTEST hTau antigen; Innogenetics, Gent, Belgium), as described elsewhere.[4] CSF-Aβ42 was also quantified with a specifically constructed sandwich enzyme-linked immunosorbent assay system.[6] The sample collection was performed after written informed consent was obtained from each participant or a family member. Demographic profiles of the patients examined in this study are summarized in Table 1.

Plasma and Cerebrospinal Fluid Neprilysin Activity Assay

Before high-throughput analysis, neprilysin in CSF was identified by immunoblotting for a subset of CSF samples with antibody against human neprilysin (goat polyclonal; 1:400 dilution; Genzyme-TECHNE, Minneapolis, MN). Lysates of murine primary cortical neurons overexpressing human neprilysin[19] were used as control samples. Subsequently, CSF-NEP in all patients was fluorometrically assayed as thiorphan-inhibitable peptidase activity, based on the previously described protocol.[14] Briefly, a 20μl CSF sample was used for enzymatic cleavage of succinyl-Ala-Ala-Phe-AMC, with or without thiorphan, a specific inhibitor of neprilysin. Similarly, plasma-NEP was biochemically quantified by using 5μl plasma samples.

The application of fluorometric assay to CSF samples was

validated by examining correlation between intensity of immunoblotting signal and measured CSF-NEP. In addition, we assessed the specificity of CSF-NEP assay by immunodepleting CSF samples with antibody against human neprilysin (Genzyme-TECHNE; goat polyclonal) and protein G agarose slurry (Oncogene/Calbiochem, Cambridge, MA). Antibody against $GABA_A$ receptor α_1 subunit (Santa Cruz, Santa Cruz Biotechnology, CA; goat polyclonal) was also used as a control antibody for immunodepletion.

Biochemical Characterization of Cerebrospinal Fluid Neprilysin

Cortical brain samples from autopsy-confirmed AD cases were homogenized with 4 volumes of 50mM tris(hydroxymethyl)aminomethane (Tris)-hydrochloride buffer (pH 7.6) containing 150mM sodium chloride (NaCl) and protease inhibitor cocktail and centrifuged at 200,000× *g* for 20 minutes at 4°C. The resultant pellet was rehomogenized with 3 volumes of the above-mentioned buffer plus 1% Triton X-100 (Sigma Labs, St. Louis, MO) and centrifuged at 200,000× *g* for 20 minutes at 4°C. The supernatant was then used for immunoblot analysis. CSF samples from the patients were processed with sodium dodecyl sulfate polyacrylamide gel electrophoresis Clean-Up Kit (Amersham Biosciences, Piscataway, NJ). Lysates of murine primary cortical neurons overexpressing human neprilysin[19] and recombinant protein corresponding to the extracellular domain of human neprilysin (Genzyme-TECHNE) were also used as control samples. In addition, aliquots of the protein samples were chemically deglycosylated by using trifluoromethanesulfonic acid.[20] The nondeglycosylated and deglycosylated protein samples (~10μg) were applied to immunoblotting with antibody against human neprilysin (Genzyme-TECHNE).

Animal Experiments

To prove the transport of neuronal neprilysin from the brain into CSF, we assayed CSF-NEP in neprilysin-deficient mice after intrahippocampal injection of recombinant adeno-associated viral vector expressing human neprilysin (rAAV-NEP), which was prepared as described elsewhere.[14] Twelve neprilysin-deficient mice (generously provided by Dr C. Gerard, Harvard Medical School), aged 18 to 20 months, were injected with 0.6μl rAAV-NEP preparations (~1.3×10^{10} genome copies) into the bilateral dentate gyri of the hippocampus (stereotactic coordinates: anteroposterior, 2.4mm; mediolateral, 2.0mm; and dorsoventral, 2.0mm). At 10 weeks after injection, the mice were anesthetized with pentobarbital, and CSF was isolated from the cisterna magna compartment under a dissecting microscope, based on the protocol by De-Mattos and colleagues.[21] CSF samples (20–30μl from each mouse) were combined into three pooled volumes. After the collection of CSF, blood sampling was performed by cardiac puncture. The mice were then transcardially perfused with phosphate-buffered saline (PBS), and the hippocampi were dissected, homogenized with 9 volumes of 50mM Tris-hydrochloride buffer (pH 7.6) containing 150mM NaCl and EDTA-free protease inhibitor cocktail, and centrifuged at 200,000× *g* for 20 minutes at 4°C. The resultant pellet was rehomogenized with 2 volumes of above-mentioned buffer plus 1% Triton X-100 and centrifuged at 200,000× *g* for 20 minutes at 4°C. The supernatant was used as solubilized membrane fraction for biochemical analyses. For comparison, CSF, plasma, and hippocampal samples were also obtained from 12 wild-type and 12 neprilysin-deficient mice, aged 20 to 22 months, that were untreated. Plasma- and CSF-NEP were measured as described earlier, and a similar experimental procedure was applied to assay for hippocampal neprilysin activity by using 10μg protein in the membrane fraction. In the plasma and hippocampal analyses, 3 of 12 mice were randomly chosen in each study group, and samples from the selected mice were used for the assays. In addition, we also performed immunoblotting of neprilysin in pooled CSF samples using antimouse neprilysin antibody (Genzyme-TECHNE; goat polyclonal). Recombinant mouse neprilysin (Genzyme-TECHNE) was used as a control.

Because neprilysin in degenerating neurons can be released into CSF due to disruption of membrane structures to which neprilysin is anchored, CSF-NEP is likely to be affected by not only the level of brain neprilysin, but also the magnitude of neurodegeneration. Hence, we examined CSF-NEP in rats after low- and high-dose administrations of kainic acid (KA), an inducer of excitotoxic insults in the CNS neurons. At 7 weeks old, nine female Sprague–Dawley rats were divided into three groups. Rats in the control group were intraperitoneally injected with PBS, and the low- and high-dose KA groups underwent intraperitoneal administration of 10 and 50mg/kg KA dissolved in PBS, respectively. CSF and blood samples were collected in the control rats and rats treated with low-dose KA at 48 hours after injection as in the mouse experiment. All rats in the high-dose KA group exhibited a lethal status epilepticus within 5 hours of injection, and CSF and blood were sampled immediately after death of the animals. After CSF and blood collections, rats in all groups were transcardially perfused with PBS, and the brains were removed. The right hemisphere was fixed overnight with 4% paraformaldehyde in phosphate buffer (pH 7.4). Protein level and enzymatic activity of neprilysin in the CSF, plasma, and hippocampal samples were quantified by immunoblotting and fluorometric assay, respectively, as described earlier. We also analyzed levels of tau in CSF by immunoblotting with anti–tau antibody (Tau-1; mouse monoclonal; Chemicon, Temecula, CA). Before immunoblotting, albumin and IgG were removed from CSF preparations using a ProteoExtract Albumin/IgG Removal Kit (Calbiochem, San Diego, CA), followed by dephosphorylation of the samples using alkaline phosphatase (Sigma). For histochemical and immunohistochemical analyses, representative 10μm frozen sections of the right hemisphere were generated. Extents of excitotoxic insults and synaptic loss were investigated by immunofluorescence staining with antibodies against calpain-cleaved α-spectrin (rabbit polyclonal)[22] and vesicular GABA transporter (117G4; rabbit polyclonal; Synaptic Systems GmbH, Goettingen, Germany), respectively. Amount of neprilysin was also examined by using antineprilysin antibody (56C6; mouse monoclonal; Novocastra Laboratories, Newcastle, United Kingdom). Immunostaining signals were amplified with a TSA-Direct kit (NEN Life Science Products, Boston, MA).

Statistical Analyses

For group comparisons of clinical and biochemical variables, one-way analysis of variance was done, followed by Bonfer-

roni multiple comparison test. Correlations between two variables were tested by the t statistic.

Results

Reduction of Cerebrospinal Fluid Neprilysin Activity in Early Stages of Alzheimer's Disease Pathogenesis

In 11 CSF samples, a close correlation between intensity of neprilysin immunoblotting signal and measured CSF-NEP was observed (Figs 1A, B). Moreover, CSF-NEP was substantially reduced by immunodepleting the samples with antineprilysin antibody (see Fig 1C). These findings justify the application of CSF-NEP assay to high-throughput analysis of CSF samples with sufficient specificity.

Quantified CSF-NEP in the control, pMCI, and AD groups is shown in Figure 1D. CSF-NEP was signifi-

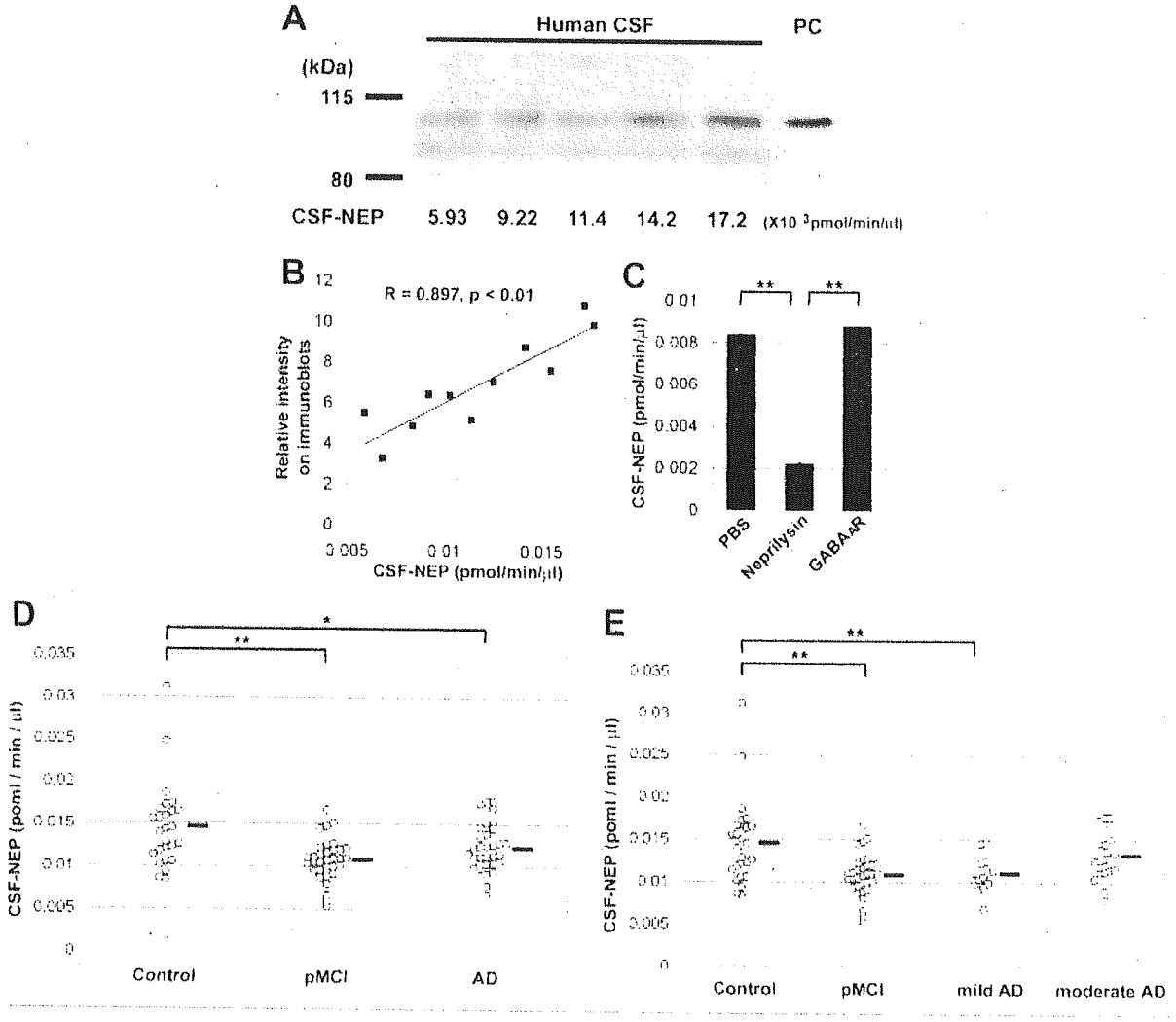

Fig 1. Decreased levels of cerebrospinal fluid neprilysin activity (CSF-NEP) in patients with incipient and mild Alzheimer's disease (AD). (A) Representative immunoblotting of neprilysin in human CSF samples demonstrates that apparent molecular mass of CSF neprilysin is nearly the same as that of the human neprilysin from primary culture (PC) of cortical neurons. The same volume of CSF preparation was loaded in each lane. CSF-NEP determined by fluorometric assay of enzymatic peptidolysis using the same sample is shown at the bottom. (B) CSF-NEP showed a close correlation with intensity of neprilysin immunoblotting signal in 11 human CSF samples. (C) CSF-NEP was reduced substantially by immunodepletion with antineprilysin antibody (neprilysin) relative to those in control subjects treated with either phosphate-buffered saline or antibody against anti–GABA$_A$ receptor α_2 subunit (GABA$_A$R). All assays were performed in triplicate. Bars *represent standard error. (D) A significant reduction of CSF-NEP was observed in patients with progressive mild cognitive impairment and AD compared with control subjects. Each* circle *represents the value obtained for a single individual, and* horizontal lines *represents the mean value in each group. (E) Patients with mild AD (Mini-Mental State Examination [MMSE] score, ≥17) showed a significant decline of CSF-NEP, whereas levels of CSF-NEP in patients with moderate AD (MMSE score, 9–17) were similar to those in control subjects. *$^*p < 0.05$; $^{**}p < 0.01$.*

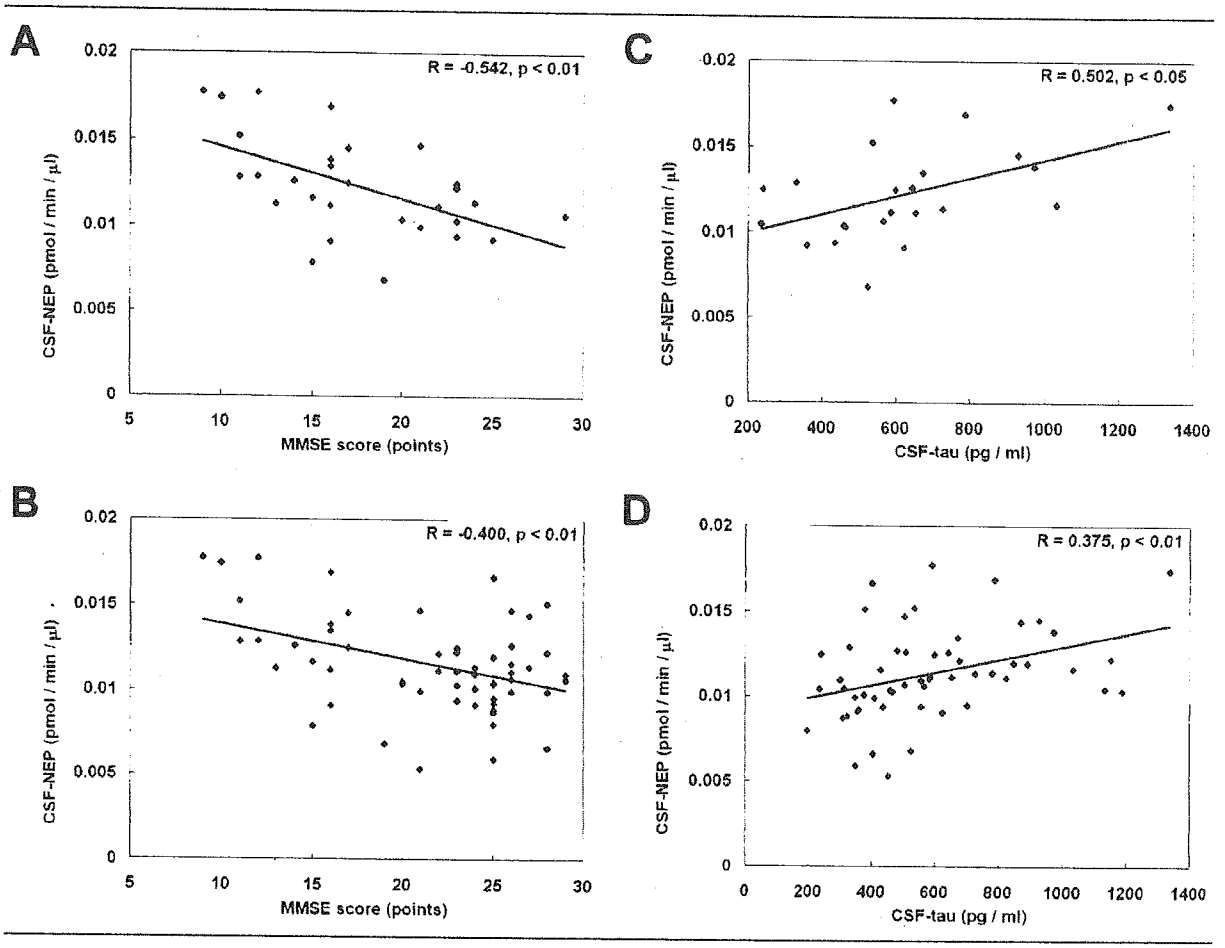

Fig 2. Association of cerebrospinal fluid neprilysin activity (CSF-NEP) (CSF-NEP) with disease severity assessed by Mini-Mental State Examination (MMSE) score and CSF-tau level in patients with progressive mild cognitive impairment (pMCI) and Alzheimer's disease (AD). (A) CSF-NEP was increased with disease progression in AD patients and was significantly correlated with MMSE score. (B) A significant correlation between CSF-NEP and MMSE score was also observed when patients with pMCI were added to the study group. (C) CSF-NEP showed a significant and positive correlation with CSF-tau in AD patients. (D) Correlation between CSF-NEP and CSF-tau levels remained significant when patients with pMCI were also included in the analysis. Solid lines *represent the linear regression of the data.*

cantly decreased in pMCI patients (0.0108 ± 0.0004pmol/min/µl; mean ± SE) compared with subjects in the control group (0.0146 ± 0.0008pmol/min/µl). There also was a significant decrease of CSF-NEP in AD patients (0.0121 ± 0.0005pmol/min/µl) compared with the control group. When the AD patients were subdivided into mild (MMSE scores, >17 points) and moderate AD groups (MMSE scores, 9–17 points), patients with mild AD showed a significant reduction of CSF-NEP (0.0107 ± 0.0006pmol/min/µl) relative to the control subjects (see Fig 1E). By contrast, CSF-NEP in patients with moderate AD (0.0132 ± 0.0007pmol/min/µl) was similar to the control level (see Fig 1E). Alteration of CSF-NEP during progression of AD was more intensively analyzed by plotting CSF-NEP data in AD patients against their MMSE scores. Notably, levels of CSF-NEP in AD patients showed a significant inverse correlation with MMSE scores (Fig 2A). The correlation remained significant after data from pMCI patients were added to the plot (see Fig 2B). Thus, it is conceivable that occurrence of a prominent CSF-NEP reduction is confined to early stages of AD pathogenesis, and thereafter CSF-NEP is likely to be reversed to greater levels with advance of the disease.

AD patients with high levels of CSF-NEP showed higher levels of CSF-tau, thus the correlation between the two variables was significant (see Fig 2C). There also was a significant correlation between CSF-NEP and CSF-tau when patients with pMCI were combined with AD patients for analysis (see Fig 2D). Because CSF-tau is supposed to increase as a function of cytoskeletal disruption and abnormal tau accumulation in neurons, these findings support an increased diffusion of neuronal

neprilysin to the extracellular matrix and CSF as a consequence of injuries of neuronal membranes.

CSF-NEP was unrelated to CSF-Aβ42 in AD patients ($R = -0.112$, $p > 0.05$; data not shown), whereas correlation between these two variables became significant when patients with AD and pMCI were included for analysis ($R = -0.262$, $p < 0.05$; data not shown).

CSF-NEP was not correlated with age and sex in any of the studied groups. In addition to the aforementioned simple correlation analyses, multiple regression with stepwise selection option was used as an exploratory tool for identification of primary factors that determine levels of CSF-NEP in patients with pMCI and AD. As listed in Table 2, MMSE score and CSF-tau were selected as independent variables. CSF-tau showed the greatest partial correlation to CSF-NEP, and MMSE score also had a tendency to be correlated to CSF-NEP. Other variables, including age, sex, and CSF-Aβ42 were eliminated by the stepwise selection; thus, it is likely that the marked influence of the disease severity on both CSF-NEP and CSF-Aβ42 produced an apparent correlation between these two CSF measures in the simple correlation analysis.

CSF-NEP in sMCI subjects (0.0147 ± 0.001pmol/min/μl) was similar to that in control subjects ($p > 0.05$) and was significantly greater than that in pMCI subjects ($p < 0.05$), implying applicability of CSF-NEP measurement to differentiation between pMCI and sMCI at baseline examination.

Neprilysin in CSF was further characterized by immunoblotting (Fig 3). Deglycosylated neprilysin in the brain and CSF showed the same molecular mass, which was larger than the apparent molecular weight of extracellular domain of neprilysin and corresponded to the predicted size of the full-length form. Therefore, secretion of neprilysin from neurons to the extracellular matrix likely occurs without shedding of the full-length enzyme.

Plasma-NEP did not differ among the control (1.669 ± 0.306pmol/min/μl), pMCI (1.777 ± 0.429pmol/min/μl), and AD (1.944 ± 0.395pmol/min/μl) groups. Patients with mild (2.036 ± 0.725pmol/min/μl) and moderate AD (1.816 ± 0.494pmol/min/μl) exhibited similar levels of plasma-NEP. Moreover, there was no significant correlation between levels of CSF-NEP and plasma-NEP in any of the examined groups ($R = 0.103$, $p > 0.05$; data not shown). Hence, the CSF-NEP changes in patients with pMCI and early AD observed in this study were unrelated to the status of plasma neprilysin, but they conceivably reflected an altered transfer of neprilysin from the brain to CSF in these patients. This notion was further tested by the following experiments using rAAV-treated, neprilysin-deficient mice and KA-treated rats.

Table 2. Multiple Regression Analysis for Patients with pMCI and AD

Independent Variable	Partial Correlation Coefficient	p
MMSE	−0.237	0.096
CSF-tau	0.292	0.042

$R^2 = 0.152$, $F = 5.93$, $p = 0.027$.
Age, sex, and CSF-Aβ42 were eliminated from independent variables by the stepwise selection.
pMCI = progressive mild cognitive impairment; AD = Alzheimer's disease; MMSE = Mini-Mental State Examination; CSF = cerebrospinal fluid.

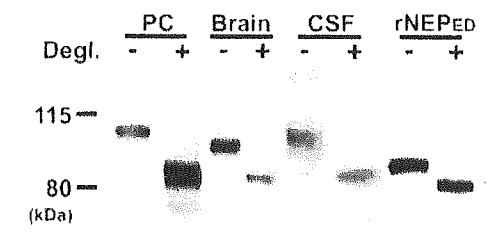

Fig 3. Biochemical characteristics of neprilysin in the brain and cerebrospinal fluid (CSF) from the human subjects. Non-deglycosylated neprilysin in the CSF sample from an AD patient migrated at approximately 95kDa, which was nearly the same as the apparent molecular mass of the human neprilysin from primary culture (PC) of cortical neurons, whereas neprilysin in the membrane-associated fraction extracted from the brain migrated slightly faster than the CSF neprilysin. After deglycosylation, the apparent molecular weight of neprilysin in the PC, brain, and CSF became approximately 85kDa, which corresponds to the predicted size of full-length, unmodified neprilysin. The recombinant extracellular domain of human neprilysin ($rNEP_{ED}$) exhibited smaller apparent molecular mass than other samples.

Physiological Transfer of Neprilysin from the Brain to Cerebrospinal Fluid Demonstrated in Mice

Neprilysin activity was assayed in the hippocampus, CSF, and plasma of neprilysin-deficient mice injected with rAAV-NEP, as well as untreated wild-type and neprilysin-deficient mice. Hippocampal neprilysin activity was nearly undetectable in the untreated neprilysin-deficient mice, whereas it prominently increased at 10 weeks after injection with rAAV-NEP (Fig 4A). There remained unnegligible signals in CSF-NEP assay for untreated neprilysin-deficient mice, which may be produced by degradation of the substrate by thiorphan semisensitive endopeptidases (see Fig 4B). In rAAV-NEP–treated, neprilysin-deficient mice, CSF-NEP showed a significant increase to approximately 70% of CSF-NEP in wild-type mice (see Fig 4B). By contrast, plasma-NEP in neprilysin-deficient mice treated with rAAV-NEP stayed at an undetectable level, similar to